Earth Systems and Environment
https://doi.org/10.1007/s41748-026-01289-y

ORIGINAL ARTICLE

Impacts of Climate Change on Offshore Wind Power Density in Brazil Under Different Warming Scenarios

Jean Souza dos Reis[1,2,4] · Fabrício Daniel dos Santos Silva[1] · Helber Barros Gomes[1] · Rafaela Lisboa Costa[1] · João Otavio Alves Accioly[1] · Mário Henrique Guilherme dos Santos Vanderlei[1] · Glauber Lopes Mariano[1] · Helder José Farias da Silva[1] · Katyelle Ferreira da Silva Bezerra[1,3] · Heliofábio Barros Gomes[1] · Madson Tavares Silva[3] · Jório Bezerra Cabral Júnior[4] · Daniele Tôrres Rodrigues[5] · Gabriel de Oliveira[6] · Malaquías Peña[7] · José Antônio Mantovani Júnior[8] · Dirceu Luís Herdies[8]

Received: 26 March 2026 / Revised: 10 June 2026 / Accepted: 13 June 2026
© The Author(s) 2026

Abstract

This study investigates the impacts of climate change on Brazil's offshore wind energy potential across the Northeast, Southeast, and South regions using projections from 27 global climate models participating in the Coupled Model Intercomparison Project Phase 6 (CMIP6) under the Shared Socioeconomic Pathways SSP1-2.6, SSP2-4.5, and SSP5-8.5 scenarios. Wind speeds were extrapolated to 100 m and used to estimate wind power density (WPD) in offshore areas currently under regulatory assessment for wind farm development. The results reveal distinct regional responses to global warming. The Northeast maintains the highest mean WPD but shows a tendency toward reduction under the high-emission scenario (SSP5-8.5), associated with the projected weakening of the trade winds. In contrast, the Southeast exhibits a consistent increase in wind potential, particularly under SSP5-8.5, suggesting a potential intensification of the resource under stronger warming conditions. In the South, projections indicate moderate increases accompanied by considerable interannual variability. Overall, mean annual changes remain below 15% across most analyzed areas, although more pronounced seasonal variations occur during specific periods. These findings suggest that global warming may reshape the regional distribution of offshore wind resources in Brazil, with important implications for long-term energy planning and offshore wind development.

✉ Fabrício Daniel dos Santos Silva
fabricio.santos@icat.ufal.br

1 Institute of Atmospheric Sciences, Federal University of Alagoas, Maceió, Brazil

2 Center for the Integration of Data and Knowledge for Health, Salvador, Brazil

3 Academic Unit of Atmospheric Sciences, Federal University of Campina Grande, Campina Grande, Brazil

4 Institute of Geography, Development and Environment, Federal University of Alagoas, Maceió, Brazil

5 Department of Statistic, Federal University of Piauí, Teresina, Brazil

6 Stokes School of Marine and Environmental Sciences, Mobile, AL, USA

7 University of Connecticut, Storrs, USA

8 National Institute for Space Research, Cachoeira Paulista, Brazil

Published online: 21 July 2026

Graphical Abstract

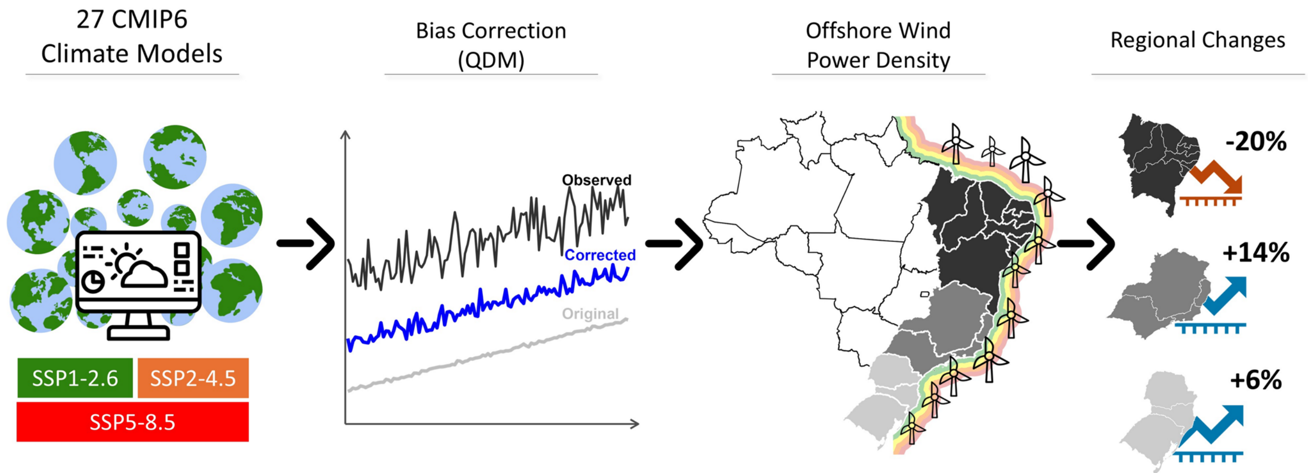

This graphical abstract presents an assessment of how climate change may affect offshore wind potential in Brazil (Northeast, Southeast, and South) using projections from 27 CMIP6 global climate models under the SSP1-2.6, SSP2-4.5, and SSP5-8.5 scenarios. The results indicate that the Northeast maintains the highest wind power density values but tends to show reductions under high-emission conditions, while the Southeast exhibits a consistent increase in wind resources and the South shows moderate increases with high interannual variability. Overall, mean annual changes remain below 15%, but they may alter the regional distribution of offshore wind resources and influence long-term energy planning in Brazil.

Highlights

- Offshore wind climate impacts assessed using 27 CMIP6 climate models.
- Bias-corrected projections applied using Quantile Delta Mapping.
- Wind power density increases up to ~ 14% offshore Southeast Brazil.
- Seasonal reductions up to ~ 20% projected in Northeast Brazil.
- Annual offshore wind changes remain below 15% in most regions.

Keywords Offshore wind energy · Wind power density · CMIP6 · Climate change · Brazil

1 Introduction

The global energy transition has accelerated in response to the urgent need to reduce greenhouse gas emissions and mitigate the impacts of climate change. In this context, renewable energy sources such as solar and wind play a central role and have evolved rapidly over the past decade, driven not only by environmental concerns but also by increasing economic competitiveness. Recent projections highlight the scale of this transformation. Global renewable power capacity is expected to double by 2030, with an expansion of approximately 4,600 GW, reflecting an unprecedented acceleration in deployment (International Energy Agency 2025). Wind energy, in particular, is projected to nearly double its installed capacity, exceeding 2,000 GW by the end of the decade, reinforcing its strategic importance in the global energy mix. At the same time, renewable technologies have reached a decisive cost-competitiveness threshold, with the levelized cost of electricity from solar photovoltaics and wind declining substantially over the last decade (International Renewable Energy Agency, 2024). The rapid expansion of renewables is also reshaping energy systems, with variable sources expected to account for an increasing share of global electricity generation, intensifying challenges related to variability, grid integration, and system flexibility (International Energy Agency 2025). In parallel, the sector has become a major driver of economic growth and employment, with global renewable energy jobs reaching approximately 16.6 million people in 2024 (International Renewable Energy Agency and International Labour Organization 2026). These trends reinforce the central role of renewable energy in achieving climate targets. More than 130 national governments have committed to significantly increasing renewable energy capacity by 2030, aligning with the Paris Agreement goal of achieving net-zero emissions by mid-century (International Energy Agency, 2024; Lin and Okoye 2023). In this context, understanding how climate change may affect wind energy resources is essential to ensure the long-term reliability and sustainability of energy systems.

Wind energy, in particular, is considered a key component in the diversification of the global energy matrix (Global Wind Energy Council 2025). In recent years, the industry has expanded through advances in offshore technologies, which offer advantages such as more consistent wind regimes and fewer land-use constraints (Hosius et al. 2023). This expansion is especially relevant in emerging economies, where economic and population growth require balancing energy security, climate mitigation, and social equity in the energy transition (van Bommel and Höffken 2023; Chipangamate and Nwaila 2024).

Brazil occupies a strategic position in this context. Over the past decade, onshore wind energy has experienced rapid expansion, driven by public policies and technological advances (Silva 2023; Nóbrega 2025). As a result, onshore wind generation currently accounts for more than 33 GW of installed capacity, representing a remarkable increase compared to 0.019 GW in 2000 (Operador Nacional do Sistema Elétrico 2025). Wind energy has also become a key component of the Brazilian electricity matrix, accounting for approximately 13.2% of total electricity supply (Empresa de Pesquisa Energética 2024a). According to the Ten-Year Energy Expansion Plan for 2034 (Empresa de Pesquisa Energética 2024b), the total installed capacity of the Brazilian electricity system, considering all energy sources, is projected to reach approximately 311 GW by 2034. Of this total, about 87% is expected to come from renewable sources and 12% from non-renewable sources, complemented by emerging components such as distributed generation, energy storage, and demand response. In this context, offshore wind development emerges as a crucial alternative to support future expansion, particularly given the expected increase in electricity demand.

Wind resource assessment is commonly performed using wind power density (WPD), a metric that represents the energy available per unit area swept by turbine blades (Manwell et al. 2010; Reboita et al. 2021; Ferreira et al. 2024). Small variations in wind speed can lead to substantial changes in WPD, directly affecting project economic feasibility (Zhang and Li 2021). For this reason, wind turbines are typically installed at heights around 100 m above the surface to reduce the influence of surface roughness on wind speed (Reboita et al. 2021).

However, several studies indicate that wind resources are sensitive to climate change, with impacts varying regionally due to changes in atmospheric pressure gradients and circulation patterns (Pryor and Barthelmie 2010, 2013; Martinez and Iglesias 2021; Zakari et al. 2022; Li 2023; Nizamani et al. 2024) These changes may alter regional wind regimes, affecting both the availability and predictability of energy generation. In North America and Europe, for instance, recent assessments show that warming scenarios may significantly modify offshore wind resources, with important implications for economic planning and energy systems (deCastro et al. 2019; Pryor et al. 2023; Li 2023). Similarly, studies in tropical and equatorial regions, including the Indian subcontinent and offshore low-wind equatorial zones, also highlight the sensitivity of wind resources to climate variability and future warming (Zakari et al. 2022; Nizamani et al. 2024).

In the South American context, Ferreira et al. (2024) conducted the first continental-scale assessment using the Coupled Model Intercomparison Project is currently in its sixth phase (CMIP6) projections, applying bias correction and statistical downscaling techniques. The study identified that regions such as Northeast and South Brazil, as well as Argentine Patagonia and northern South America, may experience increases of up to 25–50% in WPD under high-emission scenarios (SSP5-8.5). However, the authors emphasize that inter-model spread is substantial, highlighting uncertainties in regional projections. Although providing a comprehensive continental overview, this study does not specifically address offshore areas under regulatory assessment in Brazil, a gap that the present research aims to fill.

Global Climate Models (GCMs) have been widely used to project such changes. The CMIP6, providing historical simulations (1850–2014) and future projections under Shared Socioeconomic Pathways (SSPs), representing the state-of-the-art in climate projections (Eyring et al. 2016; Riahi et al. 2017). These models enable the evaluation of both observed climate variability and potential impacts driven by global change (Zhang and Li 2021; Miao et al. 2023).

Despite their relevance, studies specifically addressing climate change impacts on offshore wind potential in Brazil remain limited, particularly in maritime areas already designated by Brazilian Institute of Environment and Renewable Natural Resources (IBAMA) for future development. Addressing this gap is essential, given that the country has exceptional natural conditions and is undergoing rapid expansion of renewable energy generation. At the same time, understanding how global warming may redistribute or reduce wind availability is crucial to ensure that energy infrastructure investments remain resilient under future climate conditions (Linsenmeier 2023).

Thus, this study aims to assess the impacts of climate change on offshore wind power density in Brazil under different warming scenarios (SSP1-2.6, SSP2-4.5, and SSP5-8.5), using 27 CMIP6 models and ERA5 reference data. It is important to note that these scenarios represent a range of plausible future pathways rather than predictions. In particular, low-emission scenarios such as SSP1-2.6 require rapid and sustained mitigation efforts and are considered challenging to achieve under current global climate policies, especially when accounting for institutional, technological, and socio-economic constraints (IPCC, 2023; Bertram et al. 2024). The analysis focuses on the Northeast, Southeast, and South regions, where offshore wind farm projects have already been proposed. Our objective is to provide technical support for regulatory and strategic decision-making to ensure the sustainable expansion of offshore wind energy in Brazil.

2 Data and Methodology

2.1 Study Area

The analysis was delimited to the official polygons provided by the IBAMA, corresponding to offshore areas currently undergoing environmental licensing for the installation of offshore wind farm complexes in Brazil. These polygons cover strategic sectors in the Northeast, Southeast, and South regions, where the largest proposals for offshore wind resource exploitation are concentrated.

The advancement of environmental licensing for offshore wind projects reflects Brazil's growing recognition as an emerging international hub for the development of this technology. According to the IBAMA (2022), the national regulatory framework for offshore projects has been developed based on international experience, particularly from European countries with a long-standing tradition in offshore wind generation, such as Germany, Belgium, Norway, Portugal, and the United Kingdom. This exchange of knowledge has guided the development of robust technical and legal frameworks aimed at ensuring regulatory certainty, attracting investment, and protecting sensitive marine ecosystems, including reefs, bird habitats, marine mammals, and artisanal fishing areas.

Another important milestone was the publication, in 2020, of the Standard Terms of Reference (ToR) for Environmental Impact Assessments (EIA/RIMA) applied to offshore wind developments (IBAMA 2020). This standardization has contributed to reducing subjectivity in the evaluation process and enhancing legal certainty, accelerating the submission of new licensing requests and signaling that Brazil is moving toward a technically robust environmental regulatory framework (IBAMA 2020).

Figure 1 illustrates the location of these IBAMA-defined areas, highlighting offshore sectors in the Northeast (red polygons), Southeast (blue), and South (green) regions. These spatial domains correspond to offshore wind projects currently under environmental licensing and are officially provided by the IBAMA, available through its public consultation platform (IBAMA 2026a, b); available at: https://www.gov.br/ibama/pt-br/assuntos/laf/consultas/mapas-de-projetos-em-licenciamento-complexos-eolicos-offshore) and associated technical documentation. These areas constitute the focus of this study, as they concentrate the most relevant initiatives for national energy planning and are expected to play a decisive role in Brazil's energy transition in the coming decades. Recent developments further highlight the advancement of offshore wind regulation in Brazil. In 2025, IBAMA issued the first preliminary environmental license for an offshore wind project in the country, marking a significant institutional milestone for the sector and reinforcing the feasibility of offshore wind development under the national regulatory framework (IBAMA 2025). While these areas already reflect regulatory and environmental screening processes, it is important to note that marine space is subject to multiple competing uses and constraints, including ecological protection zones, shipping routes, fisheries, and other strategic activities. These factors are not explicitly incorporated into the present analysis, and future studies should integrate wind resource assessments with marine spatial planning frameworks to provide a more comprehensive and operational evaluation of offshore wind development potential.

2.2 Climate Data Sets

In this study, monthly wind data at 10 m height from 27 GCMs (Table 1) participating in the sixth phase of the Coupled Model Intercomparison Project (CMIP6) were used (Eyring et al. 2016). For each model, a single ensemble member (r1i1p1f1, or the closest available variant when not available) was selected to ensure consistency across the multi-model ensemble. All simulations include the historical period (1850–2014) and future projections (2015–2100) under three distinct radiative forcing scenarios: SSP1-2.6, SSP2-4.5, and SSP5-8.5 (Riahi et al. 2017), following the standard CMIP6 experimental design. The spatial resolution of each model is provided in Table 1 (horizontal grid), and the analysis is based on monthly data.

The Coupled Model Intercomparison Project is currently the leading international framework for the comparative evaluation of global climate models. Established more than two decades ago as a platform for analyzing early coupled ocean–atmosphere models (Meehl et al. 1997), the project has evolved continuously and is now in its sixth phase, known as CMIP6. This latest generation of simulations provides more detailed and consistent datasets for investigating climate variability and future projections and is widely used to support the assessment reports of the Intergovernmental Panel on Climate Change (IPCC) (Eyring et al. 2016).

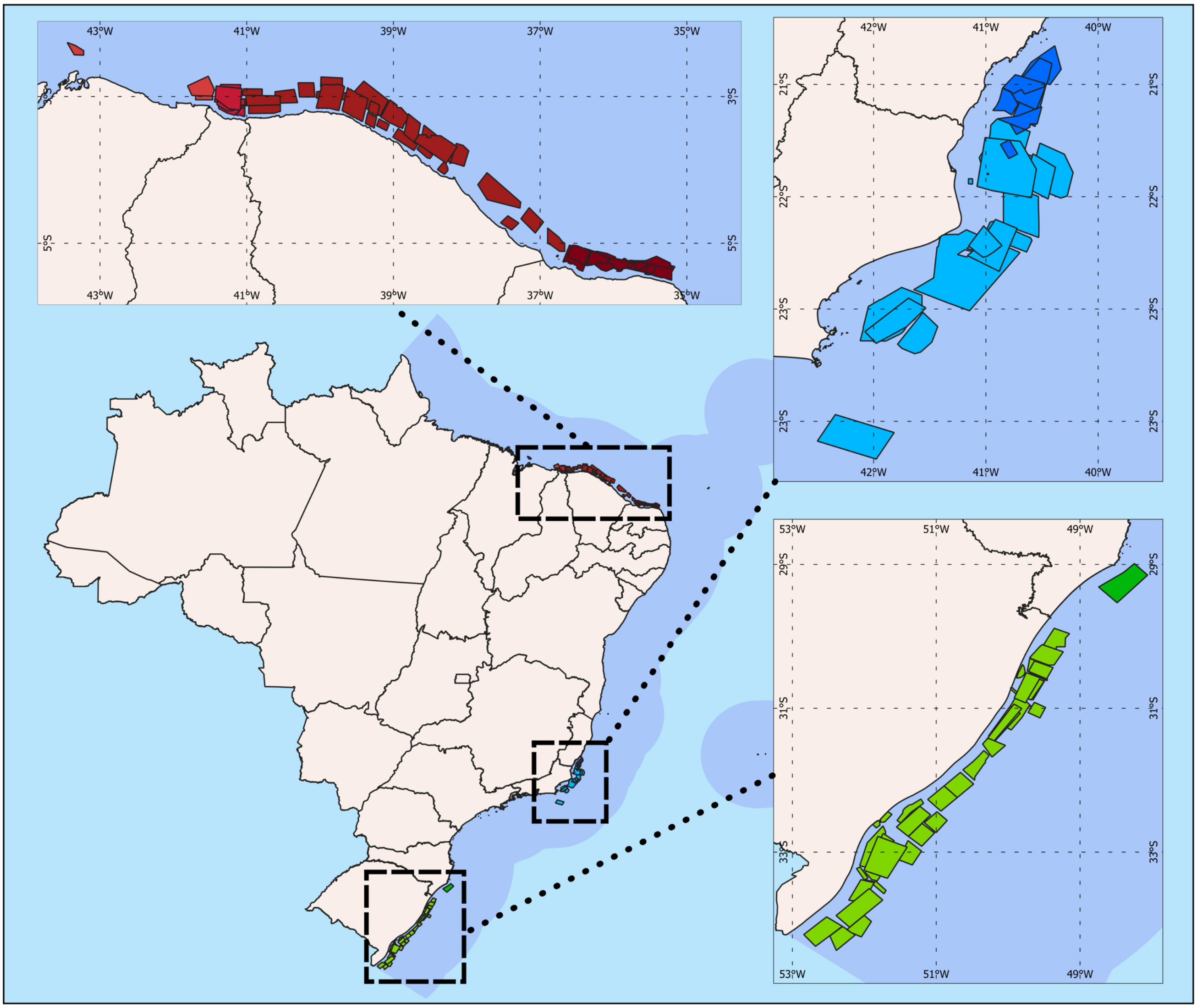

Fig. 1 Location of the official IBAMA polygons designated for environmental licensing of offshore wind complexes in Brazil. The enlarged panels highlight the three priority regions: Northeast (in red), Southeast (in blue), and South (in green). These areas represent the maritime sectors with the greatest interest for future offshore wind developments and constitute the basis for the analysis performed in this study

Each model exhibits specific characteristics in terms of spatial resolution, physical parameterizations, and representation of atmospheric circulation. These structural differences explain the variability among individual model outputs and highlight the importance of employing a multimodel ensemble (MME), which helps reduce biases and provides more robust estimates of climate variability (Zhang et al. 2023; Miao et al. 2023). The ensemble approach is widely applied in wind resource studies, as combining multiple models improves the representation of circulation patterns and wind extremes compared to individual simulations (Martinez and Iglesias 2021; Moradian et al. 2022).

The relevance of CMIP6 for the energy sector has been demonstrated in recent studies. Ferreira et al. (2024), for example, analyzed projections from eight GCMs over South America and identified increases of up to 50% in wind power density in parts of Brazil, although with substantial intermodel spread. This uncertainty underscores the importance of incorporating as many GCMs as possible, as adopted in this study, in order to capture the full range of available projections and provide more robust support for the assessment of offshore wind resources in Brazil.

2.3 Reference Data

The lack of continuous long-term wind measurements over Brazilian offshore areas represents a significant limitation for characterizing national offshore wind potential. Unlike

Table 1 Climate models used in this study, including the responsible modeling center, horizontal grid resolution, and reference

Model name	Modelling centre (Country)	Horizontal grid	Reference
ACCESS-CM2	CSIRO (Australia)	1.25° × 1.875°	(Bi et al. 2020)
ACCESS-ESM1.5	CSIRO (Australia)	1.875° × 1.25°	(Ziehn et al. 2020)
BCC-CSM2-MR	Beijing CC (China)	1.125° × 1.125°	(Xiao-Ge XIN et al. 2019)
CAMS-CSM1-0	CAMS (China)	1.125° × 1.125°	(Rong et al. 2018)
CanESM5	CCCma (Canada)	2.8125° × 2.79°	(Swart et al. 2019)
CESM2	NCAR (USA)	1.25° × 0.94°	(Danabasoglu et al. 2020)
CMCC-CM2-SR5	CMCC (Italy)	1.25° × 0.94°	(Cherchi et al. 2019)
CNRM-CM6-1	CNRM (France)	1.4° × 1.4°	(Voldoire et al. 2019)
CNRM-ESM2-1	CNRM (France)	1.4° × 1.4°	(Séférian et al. 2019)
FGOALS-g3	CAS (China)	2.25° × 2.0°	(Zhou et al. 2018)
FIO-ESM-2–0	QNLM (China)	1.1° × 0.27°–0.54°	(Bao et al. 2020)
GFDL-ESM4	GFDL (USA)	1.25° × 1.0°	(Dunne et al. 2020)
GISS-E2-1-G	NASA (USA)	2.5° × 2.0°	(Kelley et al. 2020)
HadGEM3-GC31-LL	UKMO (UK)	1.875° × 1.25°	(Williams et al. 2018)
INM-CM5-0	INM (Russia)	2.0° × 1.5°	(Volodin and Gritsun 2018)
IPSL-CM6A-LR	IPSL (France)	2.5° × 1.27°	(Boucher et al. 2020)
KACE-1–0-G	NIMS-KMA (South Korea)	1.25° × 0.94°	(Byun et al. 2019)
KIOST-ESM	KIOST (South Korea)	2.0° × 1.5°	(Pak et al. 2021)
MIROC6	MRI (Japan)	1.4° × 1.4°	(Tatebe et al. 2019)
MIROC-ES2L	MRI (Japan)	2.8125° × 2.79°	(Hajima et al. 2020)
MPI-ESM1-2-LR	MPI (Germany)	1.875° × 1.865°	(Mauritsen et al. 2019)
MRI-ESM2-0	MRI (Japan)	1.125° × 1.121°	(Kawai et al. 2019)
NESM3	NUIST (China)	1.875° × 1.865°	(Cao et al. 2018)
NorESM2-LM	NorESM (Norway)	2.5° × 1.895°	(Seland et al. 2020)
NorESM2-MM	NorESM (Norway)	1.25° × 0.942°	(Seland et al. 2020)
TaiESM1	AS-RCEC (Taiwan)	1.125° × 1.125°	(Lee et al. 2020)
UKESM1-0-LL	UKMO (UK)	1.875° × 1.25°	(Sellar et al. 2019)

in European countries, where measurement campaigns using fixed towers and lidar systems are routinely conducted, such efforts in Brazil remain limited. A recent example is the Bravo project (Remote Buoy for Offshore Wind Assessment), developed by Petrobras in partnership with the SENAI Institute for Innovation in Renewable Energies (ISI-ER) and the SENAI Institute for Innovation in Embedded Systems (ISI-SE). Although innovative, this initiative is still limited in spatial and temporal coverage and is not yet sufficient to support long-term assessments.

In this context, atmospheric reanalysis products are essential to provide a robust reference for comparison and validation of climate projections. Among the available datasets, ERA5 is currently the most advanced reanalysis produced by the European Centre for Medium-Range Weather Forecasts (ECMWF). It represents the fifth generation of global reanalyses developed by ECMWF, succeeding ERA-Interim (Dee et al. 2011), and incorporates substantial improvements in data assimilation, spatial and vertical resolution, and temporal coverage (Hersbach et al. 2020).

For this study, the following ERA5 variables were used: zonal (u) and meridional (v) wind components at 10 m and 100 m. The 100 m height was selected because ERA5 provides wind products directly at this level, allowing methodological consistency between validation, bias correction, and future projections. In addition, 100 m is widely adopted as a representative hub height in offshore wind energy assessments and corresponds to the operational range of modern wind turbines. The data were obtained at a spatial resolution of 0.25° × 0.25° (~31 km), with hourly temporal resolution, covering the period from January 1940 to December 2014. The temporal window was selected to match the historical period of the CMIP6 models, which extends until December 2014, ensuring methodological consistency between assimilated observations and climate projections.

Hourly wind components were used instead of pre-aggregated monthly values because the magnitude of the vector-mean wind (computed from monthly mean u and v) is not equivalent to the mean wind speed. Using monthly mean components can introduce directional cancellation effects associated with intra-monthly variability, particularly in regions influenced by transient systems such as cold fronts and extratropical cyclones. This effect may lead to a systematic underestimation of mean wind speed. Therefore, wind speed was first calculated at an hourly scale and subsequently aggregated to daily and monthly time scales. This approach preserves high-frequency variability and provides more robust estimates of mean wind intensity, especially in the Southeast and South regions of Brazil, where atmospheric circulation exhibits greater synoptic variability.

The choice of ERA5 is justified not only by its temporal and spatial coverage but also by its demonstrated performance in wind and wind energy studies across different regions worldwide (Reboita et al. 2021; Ferreira et al. 2024). This dataset serves as a reliable observational reference, enabling the evaluation of climate model performance during the historical period and supporting the analysis of projected future changes in offshore wind power density.

2.4 Bias Correction and Statistical Downscaling

GCMs have relatively coarse spatial resolution, which limits their direct application in regional and sectoral studies, such as those related to energy resource assessment and local climate impacts. A widely adopted approach to overcome this limitation is the application of statistical downscaling methods, which establish statistical relationships between climate model outputs and observational or reanalysis reference data (Lee and Singh 2018).

Statistical downscaling methods can be broadly classified into three main categories: (i) transfer function or regression models, (ii) stochastic weather generators, and (iii) weather typing approaches based on atmospheric pattern classification (Lee and Singh 2018). In this study, the transfer function-based method was adopted, which establishes direct statistical relationships between GCM-simulated variables and reference data. This choice is mainly justified by the ability of such methods to preserve projected temporal trends while maintaining relatively simple and robust implementation (Cannon et al. 2015). This approach is widely known as Bias Correction–Statistical Downscaling (BCSD).

In this work, statistical downscaling via bias correction was applied to monthly surface wind speed (sfcWind) data from CMIP6 models. Bias correction was performed using the Quantile Delta Mapping (QDM) technique, as proposed by Cannon et al. (2015), with historical simulations from 1995–2014 used as the training period. According to Cannon et al. (2015), QDM preserves relative changes and projected trends while correcting systematic biases in the distribution of simulated variables relative to observations. The procedure follows the univariate BCSD framework adopted in the ISIMIP2b protocol, with the distinction that a parametric formulation of distributions was employed, as proposed by Lange (2019), to enhance statistical stability in wind speed correction.

Prior to bias correction, spatial disaggregation of climate fields was performed. All CMIP6 model outputs and the ERA5-based reference dataset were interpolated onto a regular 0.5°×0.5° grid using bilinear interpolation. This method was selected due to its suitability for spatially smooth and correlated variables, such as wind speed, and its ability to generate spatially consistent fields without introducing artificial small-scale variability. Several studies have demonstrated the adequacy of this approach for continuous atmospheric variables in statistical downscaling applications (Mukherjee et al. 2018; Lee et al. 2019; Mishra et al. 2020; Xu et al. 2021; Tang et al. 2022; Wu et al. 2022; Ballarin et al. 2023; Admasu et al. 2023; Tran-Anh et al. 2023).

After spatial disaggregation, bias correction was applied using the QDM method, which follows three fundamental steps (Cannon et al. 2015). First, the trend component is isolated from the projected model distributions. Second, detrended quantiles are corrected relative to the reference data using quantile mapping techniques. Finally, the projected changes are reintroduced into the corrected values, ensuring preservation of both trends and relative changes.

Formally, let o and p denote observed (reference) and projected model data, respectively, and h and f represent the historical and future periods. Let $F_{p,h}$ and $F_{p,f}$ be the cumulative distribution functions (CDFs) of the model in the historical and future periods, respectively, and $F_{o,h}$ the CDF of the observations.

The QDM method preserves projected changes in quantiles by applying a multiplicative change factor derived from model simulations to the corresponding observed quantiles. For a given non-exceedance probability p, the bias-corrected future value $\widehat{x}_{p,f}$ is given by:

$$\widehat{x}_{p,f} = F_{o,h}^{-1}(p) \times \frac{F_{p,f}^{-1}(p)}{F_{p,h}^{-1}(p)} \tag{1}$$

where F^{-1} denotes the inverse CDF (quantile function). This formulation ensures that relative changes in quantiles simulated by the climate models are preserved after bias correction. For sfcWind, a multiplicative formulation was adopted, as recommended for strictly positive variables (Cannon et al. 2015; Lange 2019).

Thus, a parametric version of QDM was implemented, consistent with the ISIMIP3BASD v1.0 methodology (Lange 2019). For each grid cell and calendar month, parametric probability distributions were fitted separately to model historical data and reference data. Although the Weibull distribution is commonly used to represent wind speed at high temporal resolution (e.g., hourly data), the present study is based on monthly wind data, for which the statistical properties differ. Given the positive and skewed nature of wind speed at this temporal scale, the lognormal distribution was adopted as the standard functional form. This choice is consistent with the ISIMIP3BASD framework and provides a flexible and numerically stable representation, reducing artifacts associated with limited sample sizes and improving correction stability, particularly for extreme quantiles (Lange 2019).

The historical period 1995–2014 was used as the training dataset for deriving transfer functions, consistent with previous studies and the reference period adopted in reports of the Intergovernmental Panel on Climate Change (IPCC 2023a, b). The correction functions derived for this period were applied to the full historical dataset and future projections, assuming bias stationarity between the historical and future periods, while preserving the climate change signal simulated by the models.

All processing was performed independently for each model, scenario, and grid cell, ensuring preservation of the spatial and temporal variability of wind speed. To address differences in spatial resolution, the ERA5 data (originally at $0.25° \times 0.25°$) were first aggregated to $0.5° \times 0.5°$, following the ISIMIP3BASD framework (Lange 2019), and retained as the reference grid for bias correction. The GCM outputs, which have heterogeneous native resolutions, were interpolated to a common grid of $1° \times 1°$ using bilinear interpolation, ensuring consistency across models and preserving large-scale spatial patterns (e.g., Gillett et al. 2016). The QDM method was then applied using ERA5 as reference, and the corrected outputs were obtained at the $0.5° \times 0.5°$ resolution of the reference dataset. This approach ensures methodological consistency and spatial comparability across datasets (Cannon et al. 2015; Lange 2019; Ferreira et al. 2024).

2.5 Model Evaluation Metrics and Multi-model Ensemble

Model performance was evaluated using four statistical metrics widely applied in climate validation studies. Bias represents the mean difference between simulated wind speeds and those derived from reanalysis, allowing the identification of systematic overestimation or underestimation of the wind resource. The root mean square error (RMSE) quantifies the magnitude of the average error by combining both bias and variability, such that lower values indicate better agreement between simulations and reference data. Temporal correlation (Cor) was used to assess the ability of the models to reproduce interannual wind variability, a key aspect for energy resource assessments that depend on the persistence of atmospheric conditions. Finally, anomalies were calculated as deviations of simulated conditions relative to the ERA5 climatology, providing a measure of the models' ability to capture long-term patterns. A more detailed methodological description of these statistical procedures can be found in Wilks (2020).

To reduce uncertainties inherent in individual climate models and obtain more robust projections, a multi-model ensemble (MME) was constructed from CMIP6 simulations. Model selection considered the availability of monthly wind data and their spatial consistency after remapping to a common regular grid of $1° \times 1°$, onto which all GCM outputs were interpolated using bilinear interpolation. Individual model performance was evaluated based on the aforementioned metrics relative to ERA5 and ERA5 adjusted using the power-law approach. Despite differences in model performance, an unweighted ensemble was adopted, in which all models contribute equally. This strategy follows widely accepted methodological recommendations (Tebaldi and Knutti 2007), avoiding biases associated with subjective weighting schemes and ensuring that the structural diversity of the model ensemble is reflected in the final projections.

2.6 Bias Correction and Statistical Downscaling

To quantify wind resources at turbine operating height, wind data from both climate models and reanalysis were extrapolated from reference levels to 100 m above the surface. This height is considered standard for modern wind turbines, as it reduces the influence of surface friction on wind intensity (Manwell et al. 2010; Burton et al. 2011). The extrapolation was performed using the logarithmic wind profile, which relates wind speed at two different heights as a function of surface roughness length and displacement height. This approach is widely used in wind resource assessment studies due to its simplicity and physical consistency, particularly in contexts with limited vertical wind profile data (Peterson and Hennessey 1978; de Assis Tavares et al. 2020, 2022; dos Reis et al. 2023; Guimarães et al. 2025). In this study, wind speed was extrapolated from 10 to 100 m as:

$$U\left(z_2\right) = U(z_1)\frac{\ln(\frac{z_2-d}{z_0})}{\ln(\frac{z_1-d}{z_0})} \tag{2}$$

where $U(z_1)$ is the wind speed at the reference height $z_1 = 10\mathrm{m}$, $U(z_2)$ is the extrapolated wind speed at the hub height $z_2 = 100\mathrm{m}$, z_0 is the surface roughness length, and d is the displacement height. For offshore conditions, a constant roughness length of $z_0 = 0.0002\mathrm{m}$ was adopted, representing open sea conditions, consistent with standard roughness classifications (Troen and Petersen 1989; Wieringa 1992) and widely used wind resource assessment frameworks such as the Global Wind Atlas 4.0 (DTU 2025). A displacement height of $d = 0$ was assumed. Additionally, a minimum roughness threshold of $z_0 = 10^{-5}\mathrm{m}$ was applied to avoid numerical instabilities. This formulation is particularly suitable for offshore environments, where surface roughness is low and relatively homogeneous.

Using wind speed time series extrapolated to 100 m, WPD was calculated. This variable represents the kinetic energy of the wind available per unit area swept by turbine blades. The calculation followed the classical formulation (Pallabazzer 1995, 2004; Mabel and Fernandez 2009; Villanueva and Feijóo, 2010; dos Reis et al. 2023):

$$WPD = \frac{1}{2}\rho U^3 \quad (3)$$

where ρ is air density (assumed constant at 1.225 kg m^{-3}) and U is the wind speed extrapolated to 100 m. It is important to note that, by assuming constant air density, future WPD values may be overestimated, as global warming is expected to reduce atmospheric density, particularly in tropical regions. The cubic relationship between wind speed and WPD highlights the importance of accurately representing wind variability, since small differences in wind speed can lead to substantial changes in estimated energy potential. However, it is important to note that WPD does not explicitly account for turbine operational constraints, such as cut-in, rated, and cut-out wind speeds. Only wind speeds within a specific operational range contribute to actual energy production and shifts in wind speed distributions under climate change may alter the frequency of winds within this range. Therefore, while WPD provides a useful first-order estimate of the available wind energy resources, it may not fully capture changes in turbine-level energy production.

3 Results and Discussion

3.1 Model Performance Evaluation and Impact of Bias Correction

Figure 2 presents a comparative analysis of climatological wind speed fields at 100 m derived from the observational reference (ERA5), uncorrected global climate model simulations (Uncorrected GCMs), and simulations after the application of the QDM bias correction and statistical downscaling method (Bias-corrected). The analysis is shown for three coastal regions of Brazil (Northeast, Southeast, and South) during the training period (1995–2014), enabling a simultaneous assessment of spatial structure, regional gradients, and the physical consistency of wind fields.

The observed fields (Fig. 2, top row) exhibit a coherent spatial pattern characterized by well-defined coastal gradients and smooth transitions between regions of higher and lower wind intensity. These patterns reflect the interaction between large-scale atmospheric circulation, coastal topography, and land–sea contrasts, which are well captured by the ERA5 reanalysis for the recent period (Hersbach et al. 2020). This spatial structure serves as a benchmark for evaluating model performance.

In contrast, the uncorrected GCM simulations (Fig. 2, middle row) show systematic discrepancies relative to the reference, including both magnitude biases and spatial distortions. In several areas, the GCM fields display overly smoothed gradients, spatial displacement of wind maxima, and unrealistic wind intensities, reflecting inherent limitations in the coarse spatial resolution of global models and their simplified representation of coastal processes and atmospheric boundary layer dynamics (Bader et al. 2008).

After applying the QDM method, the bias-corrected wind fields (Fig. 2, bottom row) show a substantial improvement in both spatial representation and wind speed magnitude. There is a clear convergence of simulated spatial patterns toward those of ERA5, with a more realistic depiction of coastal gradients and a reduction in systematic biases present in the uncorrected simulations. This improvement is consistent with the objective of QDM, which adjusts the statistical distribution of variables while preserving the projected climate change signal (Cannon et al. 2015).

This enhancement is observed across all three regions, although the magnitude of correction varies regionally, reflecting differences in atmospheric regimes and geographic complexity. Nevertheless, it is important to emphasize that bias correction methods operate on statistical distributions and do not replace the explicit representation of physical processes, requiring careful interpretation, particularly when extrapolated to future conditions (Maraun 2016; Maraun et al. 2017).

Overall, Fig. 2 demonstrates that statistical downscaling using QDM not only improves the statistical distribution of wind time series but also enhances the spatial coherence of climatological wind fields. These results support the use of bias-corrected datasets in applications sensitive to wind spatial structure, such as offshore wind resource assessments and regional climate impact studies, while highlighting the limitations of directly using uncorrected GCM outputs.

Figure 3 presents the monthly evolution of mean wind speed at 100 m, spatially averaged over offshore regions of Northeast, Southeast, and South Brazil for the period 1995–2014. Results are shown for uncorrected CMIP6 simulations and after the application of statistical bias correction using the QDM method, with ERA5 as the reference dataset. Yellow lines represent individual ensemble members, while the black line denotes the multi-model ensemble (MME) mean.

In the uncorrected simulations, systematic biases are evident in both the mean magnitude and the amplitude of the seasonal wind cycle, with notable regional differences. This behavior is consistent with known limitations of global climate models in adequately representing boundary layer

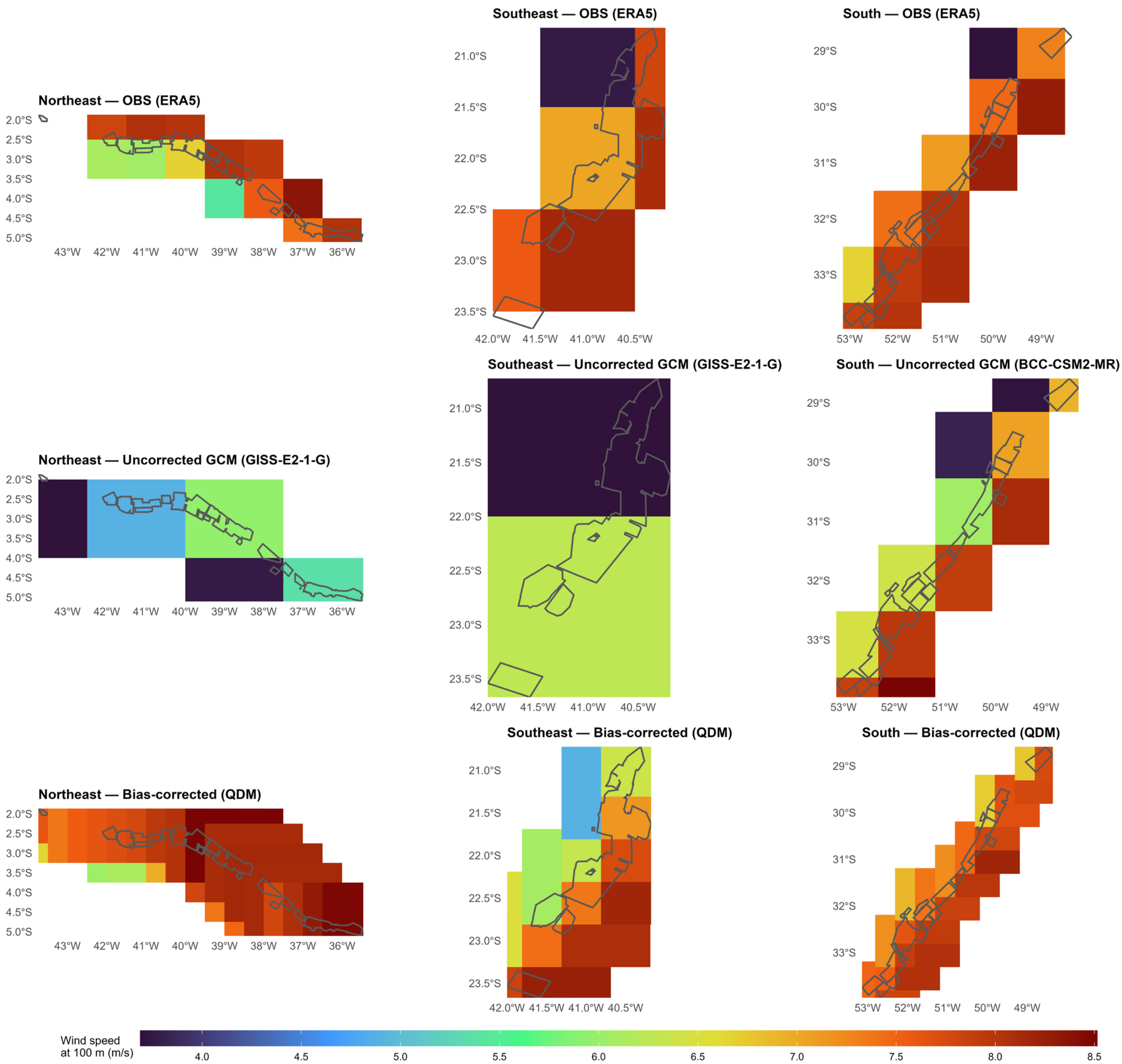

Fig. 2 Climatological mean wind speed at 100 m over Brazilian offshore regions (1995–2014). Columns show the Northeast, Southeast, and South regions. Rows represent ERA5 (top), uncorrected CMIP6 simulations (middle), and bias-corrected simulations using QDM (bottom). Colors indicate wind speed (m s^{-1}); grey contours mark offshore planning areas

processes and coastal gradients, particularly at typical GCM resolutions (Bader et al. 2008).

In the Northeast, where wind regimes exhibit strong seasonality associated with trade winds and the seasonal migration of the Intertropical Convergence Zone (ITCZ), models tend to show consistent deviations from ERA5, as well as substantial inter-model spread. This reflects structural uncertainties related to differences in physical parameterizations and model configurations (Pryor and Barthelmie 2010). In the Southeast and South regions, although mean biases are less pronounced, persistent discrepancies remain in monthly variability and in the phase of the seasonal cycle, especially during periods of enhanced synoptic variability associated with the South Atlantic Subtropical High and the passage of cold fronts and extratropical systems (Gan and Rao 1991; de Castro and de Miranda 1998).

After applying QDM, a substantial improvement in model performance is observed across all regions. The corrected MME shows significantly better agreement with ERA5, with a consistent reduction in mean bias and improved representation of both the amplitude and phase of the seasonal cycle. This behavior is consistent with the literature, which

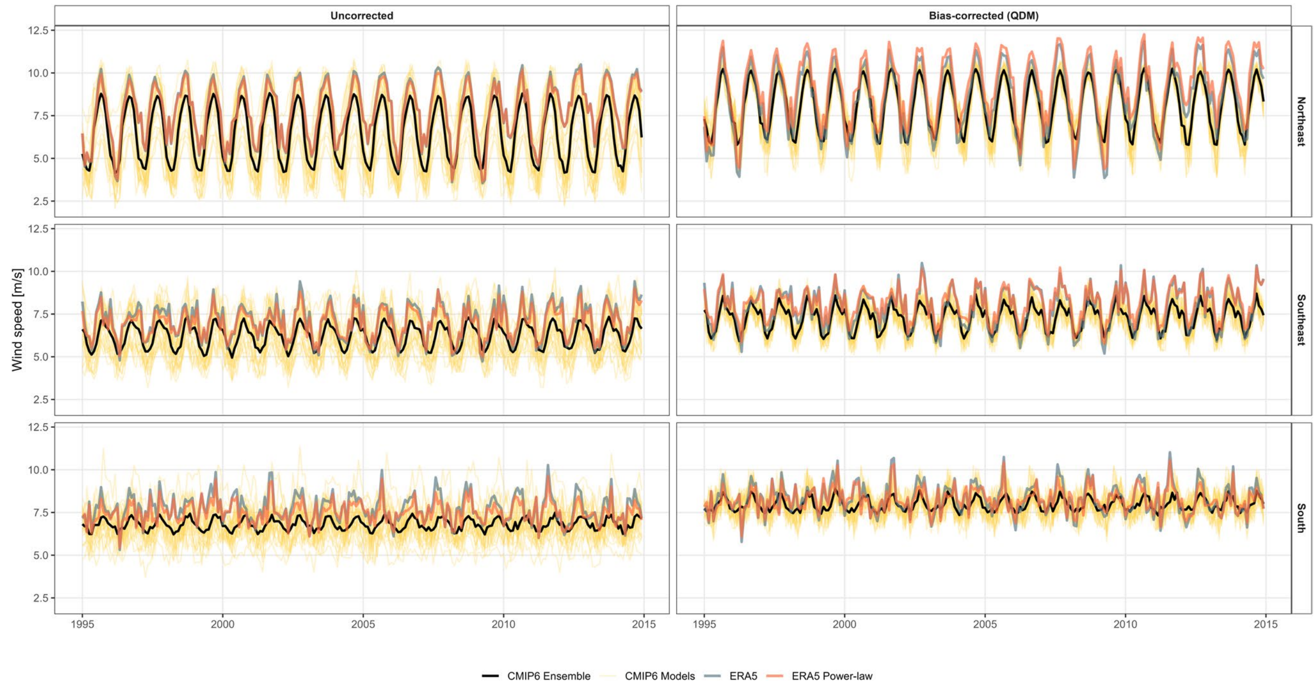

Fig. 3 Monthly evolution of mean wind speed at 100 m (m s^{-1}), spatially averaged over the offshore regions of Northeast, Southeast, and South Brazil for 1995–2014. The left column shows uncorrected CMIP6 simulations, while the right column presents bias-corrected results using QDM. Yellow lines represent individual CMIP6 models, the black line the multimodel ensemble mean (MME), the blue line ERA5, and the orange line ERA5 extrapolated using the power law

demonstrates that quantile mapping-based methods, including QDM, are effective in correcting distributions while preserving projected climate change signals (Cannon et al. 2015; Maraun 2016).

It is important to note that, despite the reduction in systematic biases, the method preserves inter-model spread, indicating that internal variability and structural differences among models are not artificially suppressed by the statistical correction—an essential feature in multi-model CMIP6 approaches (Eyring et al. 2016). Regional responses to bias correction are not homogeneous. The Northeast shows the largest relative improvements after QDM, consistent with the strong influence of large-scale seasonal forcing on regional wind regimes and the well-documented skill of ERA5 in reproducing wind patterns along the northeastern coast (Hersbach et al. 2020; Gurgel et al. 2024). In the Southeast, improvements are moderate, possibly reflecting the greater complexity of atmospheric systems and the combined influence of subtropical circulation and frontal systems. In the South, adjustments are more subtle, reflecting the relatively better performance of uncorrected models, a result also reported in regional assessments based on mesoscale models (Tuchtenhagen et al. 2020).

Overall, these results demonstrate that QDM-based statistical correction is effective in reducing systematic biases in CMIP6 wind simulations at 100 m, improving consistency with observational reference data while preserving temporal variability and model uncertainty. These aspects are particularly relevant for applications in wind resource assessment, climate impact studies, and future projections, where accurate representation of both mean conditions and variability is essential.

Figure 4 shows the variation in absolute error of wind speed at 100 m associated with the application of QDM-based statistical bias correction, relative to uncorrected CMIP6 simulations, using ERA5 as the reference dataset for the period 1995–2014. For each model and offshore region, the figure presents the monthly distribution of performance gains or losses induced by the correction, quantified as the difference between absolute errors before and after adjustment.

In this analysis, for each CMIP6 model, region, and grid point, the error difference was computed as:

$$\Delta error = |V_{Bias-corrected(QDM)} - V_{ERA5}| - |V_{Uncorrected} - V_{ERA5}| \tag{4}$$

where V_{ERA5} represents wind speed at 100 m from reanalysis, $V_{\text{Uncorrected}}$ corresponds to wind speed from the GCM without correction, and $_{V\text{Bias-corrected (QDM)}}$ denotes wind speed after QDM bias correction. Calculations were performed for the period 1995–2014. Negative values of Δerror indicate a reduction in error after bias correction, values equal to zero indicate no significant improvement, and positive values indicate an increase in error. To further evaluate the

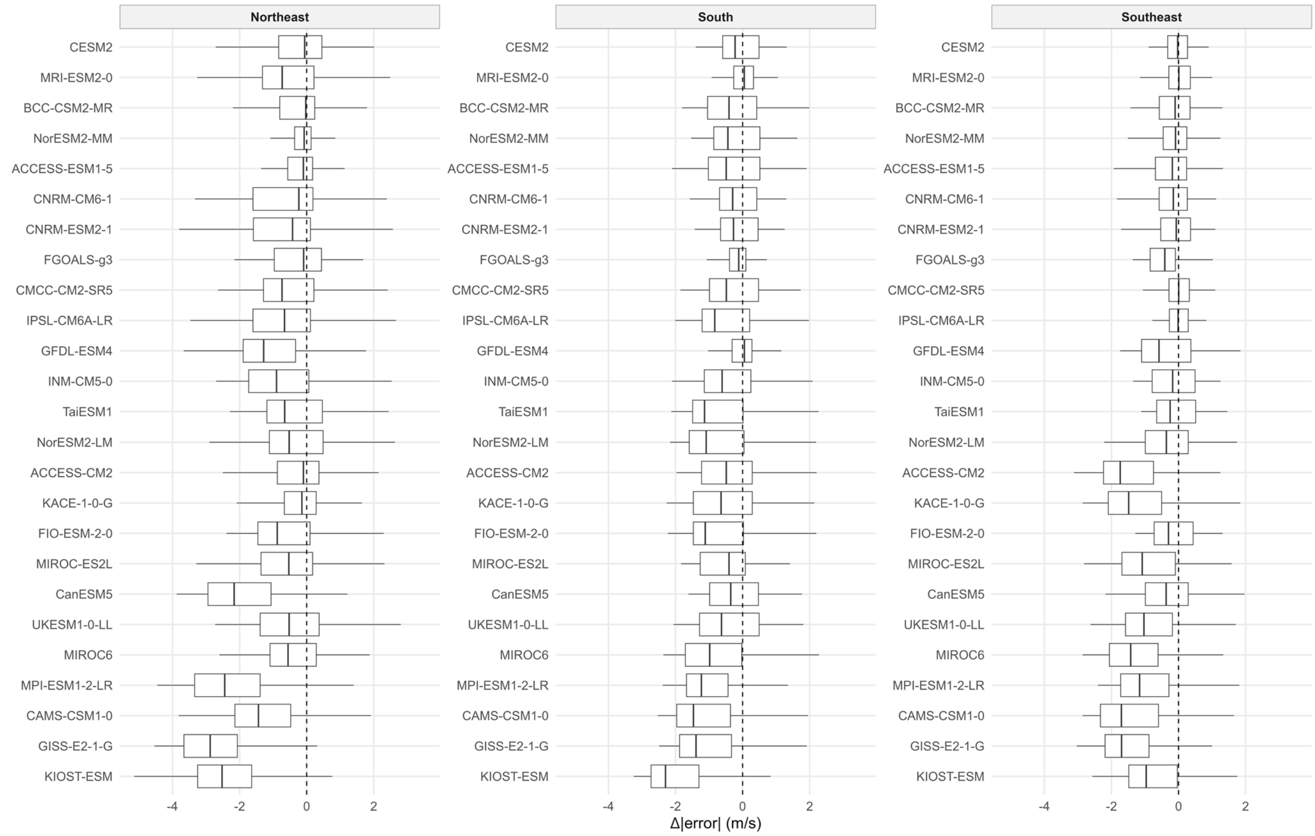

Fig. 4 Change in absolute error (Δ|error|, m s^{-1}) of 100 m wind speed after bias correction using Quantile Delta Mapping (QDM) in CMIP6 models, with ERA5 as reference (1995–2014). Panels represent the offshore regions of Northeast, Southeast, and South Brazil. Boxplots show the monthly distribution of $\Delta|\text{error}| = |\text{error}|_{(\text{uncorrected})} - |\text{error}|_{(\text{QDM})}$ for each model. Positive values indicate error reduction after correction, while negative values indicate degradation. The dashed vertical line marks the neutral condition ($\Delta|\text{error}| = 0$)

performance of the bias correction, the error reduction was analyzed across different quantiles of the wind speed distribution (Q05, Q25, Q50, Q75, and Q95). The results indicate that the QDM method improves the representation of most quantiles, particularly in the lower and median ranges. However, a larger spread in the upper quantiles suggests increased uncertainty in the correction of extreme values. This behavior is consistent with the expected performance of quantile-based bias correction methods.

Overall, QDM correction predominantly results in a reduction of absolute error across most models and regions, as indicated by negative medians of the Δ|error| metric. This behavior demonstrates the effectiveness of the method in bringing model simulations closer to observed climatology while preserving the inherent temporal variability of the series. In the Northeast, characterized by a strongly seasonal and high-intensity wind regime, improvements are more pronounced and consistent across models. Most boxplots exhibit substantially negative medians, suggesting that bias correction is particularly effective in regimes dominated by large-scale atmospheric forcing, where model biases tend to be more systematic.

In the Southeast, results indicate a moderate reduction in absolute error, with greater inter-model spread. Some models show robust improvements, while others exhibit more modest or near-neutral changes. This heterogeneity reflects the greater dynamical complexity of the region, where wind variability is influenced by interactions among synoptic systems, coastal topography, and regional thermal gradients, making bias correction less uniform.

In the South, although most models also show reduced error after QDM application, greater variability in improvement magnitude is observed, along with isolated cases of performance degradation. These results suggest that in regions where models already perform relatively well in their uncorrected state, bias correction may produce subtler adjustments and, in some cases, introduce localized temporal inconsistencies.

The intra-model spread observed across all panels indicates that the impact of bias correction is not temporally uniform, reflecting seasonal differences in bias magnitude and correction efficiency. Nevertheless, the predominance of negative Δ|error| values reinforces the robustness of

QDM as a statistical correction strategy for offshore wind resource applications.

Overall, these results demonstrate that QDM-based bias correction consistently improves the performance of CMIP6 wind simulations relative to ERA5, with regionally differentiated gains. This step is therefore essential for increasing the reliability of future wind projections and wind power density estimates, particularly in studies focused on energy planning and climate impact assessments in the offshore sector.

Figure 5 presents the evaluation of CMIP6 model performance in representing wind speed at 100 m relative to ERA5 for the historical period (1995–2014), considering three regions (Northeast, Southeast, and South). Three complementary metrics are shown (Bias, RMSE, and Correlation) for both uncorrected (Uncorrected) and QDM bias-corrected (Bias-corrected) fields.

In the uncorrected fields, a systematic pattern of negative bias is observed across nearly all models and regions, indicating an underestimation of wind speed relative to ERA5. This behavior is particularly pronounced in the Northeast and South, where several models exhibit biases lower than -1 m s^{-1}. Inter-model heterogeneity is also high, reflecting significant structural differences in the representation of wind at turbine-relevant heights among GCMs. RMSE values in the uncorrected data reinforce this pattern, showing large mean errors and considerable variability across models, especially in the Northeast and Southeast. Some models exhibit RMSE values exceeding 2 m s^{-1}, highlighting important limitations for direct energy applications without post-processing.

After applying QDM bias correction, a substantial and widespread reduction in bias is observed, with values clustering near zero across all regions. Inter-model spread is markedly reduced, indicating that the method effectively removes persistent systematic errors in global models. Consistently, RMSE shows a pronounced decrease after correction, with more homogeneous values across models and typically below 1.2 m s^{-1} in all regions. This reduction reflects not only the correction of mean bias but also an improvement in the representation of temporal variability at monthly scales.

In contrast, temporal correlation between GCMs and ERA5 is already high in the uncorrected data, with values generally exceeding 0.7 across all regions, suggesting that models adequately capture large-scale temporal variability. The application of QDM preserves this signal, resulting in only marginal changes in correlation coefficients. This behavior is expected, as QDM primarily adjusts the statistical distribution of values rather than the temporal phase of the time series.

Taken together, these results demonstrate that QDM-based bias correction substantially improves the statistical quality of wind fields by reducing both systematic and random errors without degrading temporal coherence. Although the primary focus of this study is the assessment of future wind potential, this step ensures a more robust foundation for analyzing climate projections and quantifying future changes in wind energy under different global warming scenarios.

Therefore, a central methodological choice of this study is the inclusion of all available models in the ensemble, including those that would traditionally exhibit lower performance in their raw form. This decision is justified by the substantial and consistent improvement observed after the application of bias correction and statistical downscaling. Independent evaluations indicate significant reductions in RMSE, systematic correction of mean bias, and improved temporal correlations between corrected data and observations. As a result, discrepancies among models are considerably reduced, yielding a more coherent and physically consistent ensemble.

3.2 Future Changes in Energy Production

Figure 6 shows the evolution of WPD (W m^{-2}) across the Northeast, Southeast, and South regions of Brazil, combining the historical period and projections under the SSP1-2.6, SSP2-4.5, and SSP5-8.5 scenarios throughout the twenty-first century. The time series represent annual ensemble means, obtained by spatially averaging offshore areas within each region and aggregating across all available models. The projection period is subdivided into near future (2015–2040), mid-century (2041–2070), and far future (2071–2100), used here solely as temporal reference intervals for interpretation. During the reference period (1995–2014), mean WPD values are approximately 375 W m^{-2} in the Northeast, 323 W m^{-2} in the South, and 265 W m^{-2} in the Southeast, consistent with previously reported wind potential estimates (Lucena et al. 2010; Pereira et al. 2013; Lima et al. 2015; da Silva et al. 2017; Reboita et al. 2018; Tuchtenhagen et al. 2020; Gurgel et al. 2024). A noticeable discontinuity is observed at the transition between the historical and future periods. This behavior reflects structural differences between the historical and scenario simulations in CMIP6, particularly due to changes in radiative forcing between experiments. In addition, the use of an MME, which combines simulations from different GCMs with distinct climatological characteristics, may amplify apparent shifts at the transition point. The QDM method preserves the modeled climate change signal and does not enforce continuity between periods, which can result in such discontinuities.

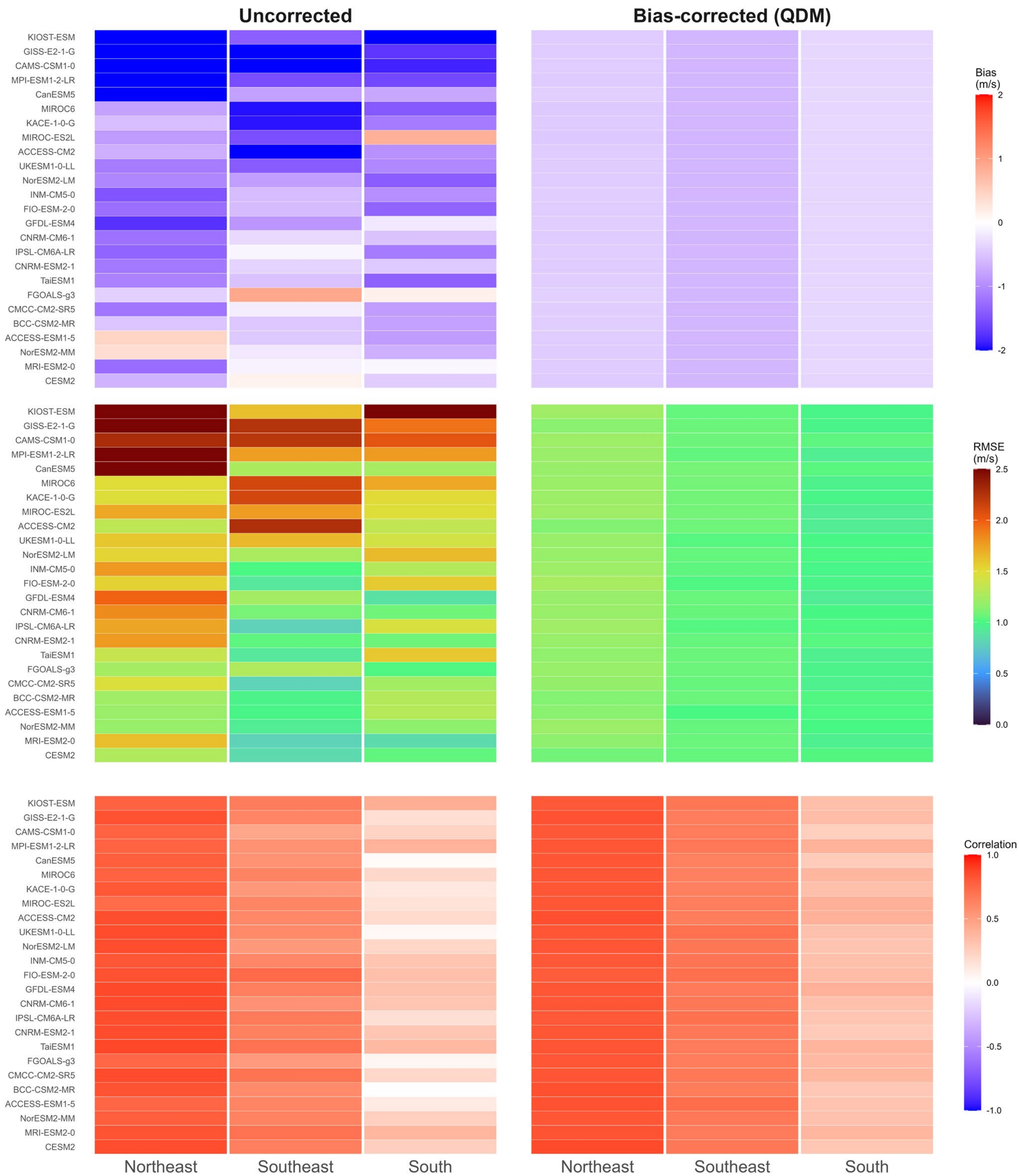

Fig. 5 Performance of CMIP6 models in representing 100 m wind speed relative to ERA5 for 1995–2014. Metrics shown for the Northeast, Southeast, and South regions include Bias (m s^{-1}), RMSE (m s^{-1}), and correlation for uncorrected and bias-corrected (QDM) simulations. Colors indicate the magnitude of each metric according to the scales shown in the panels

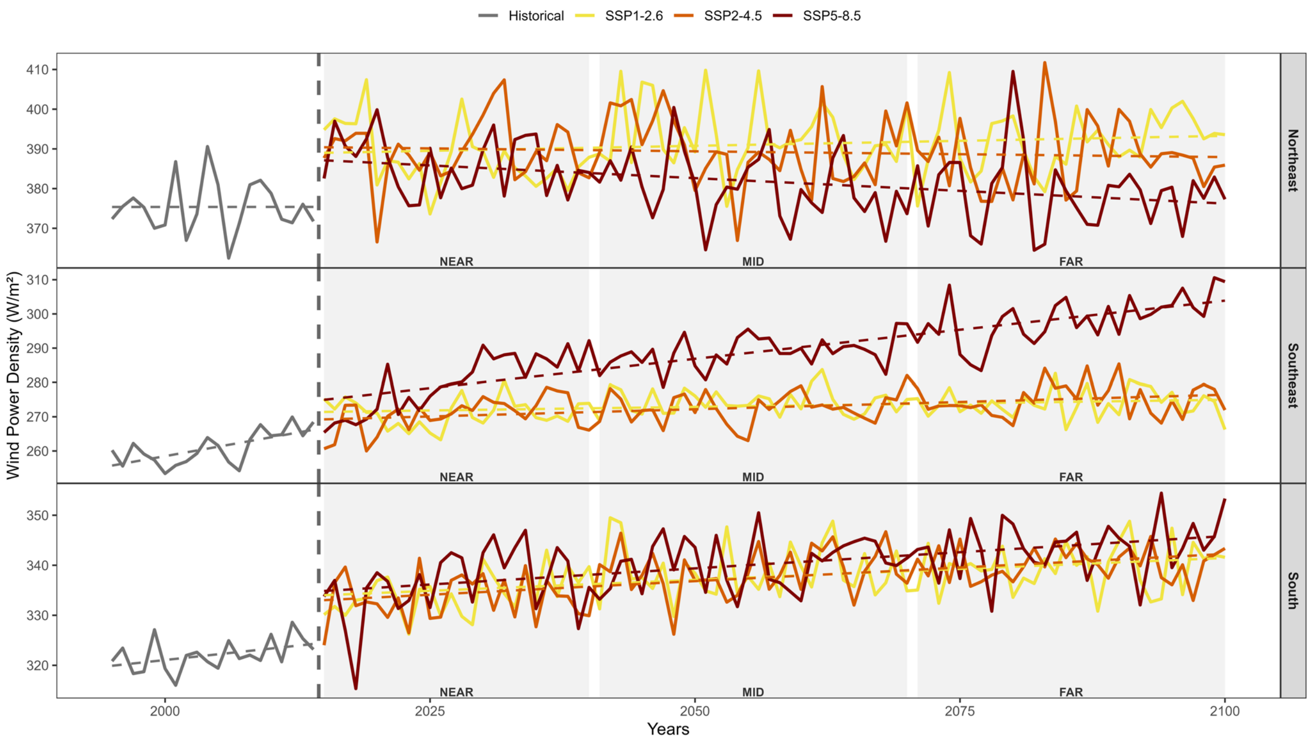

Fig. 6 Temporal evolution of 100 m wind speed (WS100, m s^{-1}) over the Northeast, Southeast, and South regions of Brazil for 2015–2100 under the SSP1-2.6, SSP2-4.5, and SSP5-8.5 scenarios. Curves represent the annual multimodel ensemble mean (MME), computed as the spatial average of each model over the regional offshore area followed by averaging across models. Results are shown separately for each region, highlighting regional differences in WS100 magnitude, variability, and response to emission scenarios throughout the twenty-first century

Overall, the Northeast exhibits the highest WPD values throughout the analyzed period, followed by the South and then the Southeast, reflecting persistent regional differences in South Atlantic wind climatology. In terms of climate change impacts, relative changes in WPD provide a more meaningful perspective, as they highlight variations in the wind resource independently of baseline conditions. Previous studies have highlighted the high wind energy potential of Northeast Brazil and its strategic importance for the national energy matrix (Lucena et al. 2010; Silva et al. 2016). Interannual variability is pronounced across all regions, particularly in the Northeast, indicating that natural variability remains significant even under different levels of climate forcing, consistent with previous multi-model assessments of wind resources (Pryor and Barthelmie 2010).

In the Northeast, relative changes in WPD remain modest under SSP1-2.6 and SSP2-4.5. Under SSP1-2.6, WPD increases by approximately + 4.5% relative to the historical period, corresponding to values ranging from ~ 390 W m^{-2} (near future) to ~ 392 W m^{-2} (far future). Under SSP2-4.5, changes remain small, at around + 3.5% throughout the century, with mean values close to ~ 388 W m^{-2}. In contrast, under SSP5-8.5, WPD shows a slight decrease, reaching approximately − 1.8% in the far future relative to the near future, associated with a reduction from ~ 385 W m^{-2} to ~ 378 W m^{-2}.

In the South, relative increases in WPD are more pronounced. Under SSP1-2.6, WPD increases by approximately + 5.9% relative to historical values, while SSP2-4.5 shows a similar magnitude of change. Under SSP5-8.5, the increase reaches approximately + 6.8%, corresponding to values up to ~ 345 W m^{-2} in the far future, indicating a consistent intensification of the wind resource across scenarios.

The mean WPD values obtained in this study for offshore areas in the Northeast and South fall within the range reported by observational and mesoscale studies. Freitas et al. (2022), based on PNBOIA buoy measurements, reported WPD values between 300 and 550 W m^{-2} in target areas such as Fortaleza (CE) and Rio Grande (RS), consistent with the historical ensemble means obtained here. Similarly, Tuchtenhagen et al. (2020), using the WRF model and BSW data, estimated an annual mean of approximately 651 W m^{-2} in the southern Exclusive Economic Zone, with seasonal peaks exceeding 1,400 W m^{-2} during winter, reinforcing that southern Brazil holds one of the highest offshore wind potentials in the country.

Dashed lines indicate long-term linear trends (2015–2100), estimated using linear regression separately for each scenario and region. In the Northeast and South, trends are relatively small compared to interannual variability, with limited differences between scenarios. CMIP6-based studies indicate that mean changes in WPD throughout the twenty-first century tend to be moderate, although strongly region-dependent and more pronounced under high-emission scenarios (Ferreira et al. 2024).

However, earlier projections based on CMIP3 models and regional downscaling suggested more pronounced increases. Pereira et al. (2013), using Eta-HadCM3 under the A1B scenario, projected increases of 15–30% in wind power density in Northeast Brazil, with peaks exceeding 100% in specific areas, particularly during autumn. Even more optimistic results were reported by Lucena et al. (2010), using HadCM3/PRECIS under A2 and B2 scenarios, indicating substantial increases in national wind potential by the end of the century, with average capacity factors rising from 17% to up to 21%. In contrast, the CMIP6 ensemble results presented here indicate more moderate and spatially heterogeneous changes, suggesting that multi-model approaches reduce the likelihood of overly optimistic projections associated with individual models.

In contrast, the Southeast shows greater sensitivity to emission scenarios, with a more pronounced positive trend under SSP5-8.5, particularly in the far future. Changes in mid-latitude atmospheric circulation and pressure gradients in the Southern Hemisphere under stronger warming scenarios are consistent with regionally differentiated wind responses (IPCC 2023a, b). Under SSP1-2.6, WPD increases from ~272 W m^{-2} (near future) to ~275 W m^{-2} (far future), representing a modest increase of approximately + 3.8% relative to historical values. Under SSP2-4.5, the evolution is similar, reaching ~274 W m^{-2} in the far future (+3.4%). However, under SSP5-8.5, the increase is substantial: WPD rises from ~280 W m^{-2} (near future) to ~302 W m^{-2} (far future), corresponding to an absolute increase of approximately + 37 W m^{-2} relative to the historical period and a relative gain of about + 14% by 2100.

The simulated mean values for the Southeast are consistent with observational and satellite-based estimates. Pimenta et al. (2008), using QuikSCAT data validated against meteorological stations, reported mean wind speeds between 6.8 and 7.4 m s^{-1} in the central region (SP–RJ) and around 8.2 m s^{-1} near Vitória (ES), corresponding to WPD values between 300 and 450 W m^{-2} in the north and approximately 600 W m^{-2} in the south. The intensification projected in this study under SSP5-8.5, particularly in offshore areas between Rio de Janeiro and Espírito Santo, is consistent with these established climatological gradients and suggests a strengthening of a previously identified high-potential wind resource core (Nogueira et al. 2023).

It is important to note that WPD depends nonlinearly on wind speed, such that small changes in wind speed at 100 m can result in amplified changes in WPD (Archer and Jacobson 2005; Pryor and Barthelmie 2010). Therefore, the linear trends presented here should be interpreted as a synthesis of the long-term mean signal. Nonetheless, linear regression provides a useful metric for comparing scenarios and regions, particularly when discussing energy planning implications across near-, mid-, and long-term horizons.

Figure 7 presents the percentage change in wind power density (ΔWPD, %) in Northeast Brazil relative to the

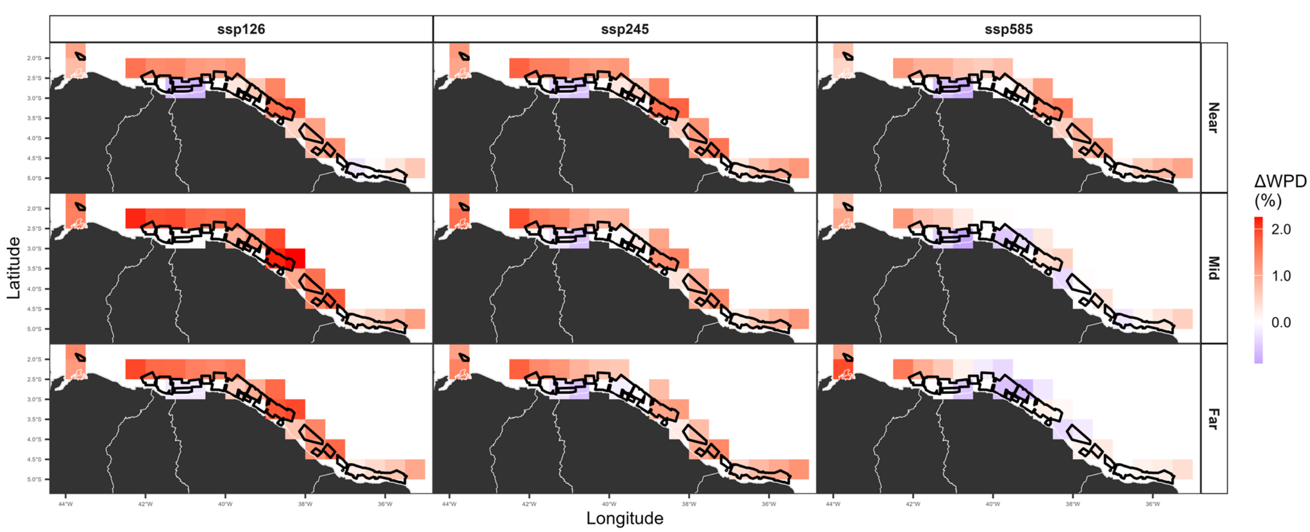

Fig. 7 Percentage change in wind power density (ΔWPD, %) over Northeast Brazil relative to the 1995–2014 reference period. Changes were computed as the difference between future and historical means for each model and grid cell, followed by the ensemble mean. Columns represent SSP1-2.6, SSP2-4.5, and SSP5-8.5 scenarios, while rows correspond to the near (2015–2040), mid (2041–2070), and far (2071–2100) future periods. Positive values indicate an increase in WPD, whereas negative values indicate a decrease relative to the historical period

reference period (1995–2014). The projected changes are spatially heterogeneous and scenario-dependent. Under SSP1-2.6 and SSP2-4.5, a pattern of modest increases predominates across most of the northeastern offshore zone. This behavior is partially consistent with continental-scale CMIP6 projections, which indicate maintenance or increases in wind potential over parts of the Northeast (Ferreira et al. 2024).

Under SSP1-2.6, projected ΔWPD (%) increases range from approximately + 0.5% to + 1.0% in the near future, reaching local peaks between + 1.5% and values exceeding + 2.0% in the mid-century period, particularly between 40°W–42°W along the coasts of Ceará and Piauí. In the far future, this increase tends to stabilize between + 1.0% and + 1.5%. Under SSP2-4.5, gains are more spatially homogeneous, remaining between + 0.5% and + 1.2% throughout the century. In contrast, under SSP5-8.5, a clear and concerning transition emerges: after modest gains between 0.0% and + 0.5% in the near future, localized reductions of up to − 0.5% appear in the mid-century period, culminating in a more widespread decrease along the eastern sector (36°W–38°W) in the far future, with reductions ranging from − 0.5% to − 1.0%. This pattern confirms that the projected weakening in the Northeast is spatially concentrated and intensifies under high-emission conditions.

Although modest increases prevail under SSP1-2.6 and SSP2-4.5, a persistent core of reduction between Piauí and Ceará is evident across all analyzed periods. This behavior partially contrasts with projections by Reboita et al. (2018), which indicated increases of 40% to 100% in wind power density under RCP8.5, particularly during autumn. This discrepancy may be attributed to methodological differences (dynamical downscaling with RegCM4 versus CMIP6 multi-model ensemble with QDM statistical correction), as well as differences in the representation of continental thermal gradients and the expansion of subtropical anticyclones. Another possible explanation lies in the regionally differentiated response of trade wind regimes to climate forcing, potentially associated with adjustments in tropical Atlantic circulation under global warming (IPCC 2023a, b).

On the other hand, the persistence of high WPD values in northern Rio Grande do Norte and Ceará is consistent with ERA5-based estimates. Gurgel et al. (2024) reported annual mean wind speeds of 7.39 m s^{-1} in northern Rio Grande do Norte and 6.78 m s^{-1} in northern Ceará, with spring peaks exceeding 9 m s^{-1}, as well as strong hydro-wind complementarity in the second half of the year (up to 79% of annual energy concentrated between July and December in northern Ceará). As discussed, under SSP5-8.5, a more pronounced relative reduction in WPD is observed in the mid- and far-future periods, accompanied by a spatial expansion of negative anomalies. Multi-model ensemble assessments indicate that higher radiative forcing scenarios tend to amplify regional contrasts in wind resource availability (Ferreira et al. 2024). Although the magnitudes remain generally moderate, differences between scenarios become more evident under SSP5-8.5. The projected reduction during austral spring in this study under SSP5-8.5 may therefore represent a significant shift in resource seasonality, with direct implications for energy security.

Figure 8 is analogous to Fig. 7 but focuses on the offshore region of Southeast Brazil. Unlike the Northeast, the Southeast exhibits a consistent spatial pattern of increasing WPD across all scenarios and periods analyzed. The projected ΔWPD (%) changes indicate that, under SSP1-2.6 and SSP2-4.5, increases remain relatively stable between + 1.0% and + 2.0% throughout the century. However, under SSP5-8.5, a more pronounced progression is observed: in the near future, increases range between + 2.0% and + 3.0%, rising to between + 4.0% and + 5.0% in the mid-century period. In the far future, projections indicate peaks exceeding + 6.0%, particularly along the northern coast of Rio de Janeiro, near approximately 21°S–40.5°W. This trajectory results in a substantial divergence between scenarios by the end of the century, reaching approximately 4–5 percentage points between SSP2-4.5 and SSP5-8.5. No extensive areas of negative anomalies are identified, indicating a robustly positive signal relative to the historical period.

This consistently positive pattern observed in the Southeast across all scenarios and time horizons is in agreement with previous regional assessments. Reboita et al. (2018) projected increased wind intensity in central-eastern Brazil (except during summer) under RCP8.5, associated with the expansion of subtropical anticyclones. Consistently, de Castro and de Miranda (1998) highlighted the role of the South Atlantic Subtropical High in modulating wind regimes along the southeastern coast, a mechanism that may be intensified under global warming scenarios. CMIP6-based studies indicate that subtropical regions of South America may experience intensification of wind resources under high-emission scenarios (Ferreira et al. 2024).

The increase is particularly pronounced under SSP5-8.5, especially in the mid- and far-future periods, consistent with projections showing stronger responses under higher warming levels (Calvin et al. 2023). Spatially, the largest increases are concentrated in offshore areas between the states of Rio de Janeiro and Espírito Santo, a region already identified as strategic for offshore wind expansion (Nogueira et al. 2023).

Figure 9, analogous to Figs. 7 and 8, presents the projected changes in offshore wind power density (ΔWPD, %) for the South region of Brazil. Overall, a predominance of positive anomalies is observed across all scenarios and time periods. Under SSP1-2.6 and SSP2-4.5, projections indicate a gradual increase in WPD, starting from values

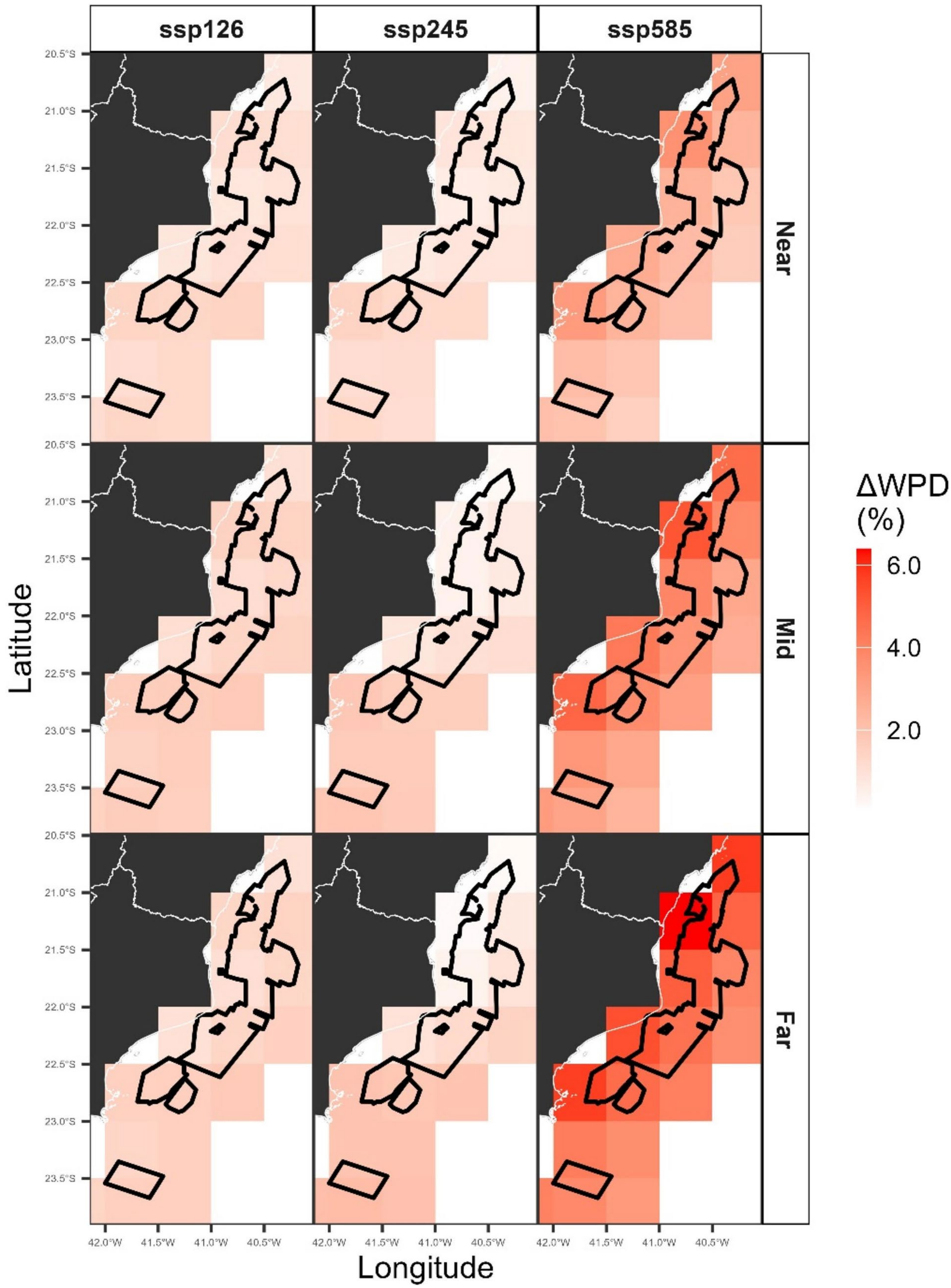

Fig. 8 Same as Fig. 7, but for the offshore region of Southeast Brazil

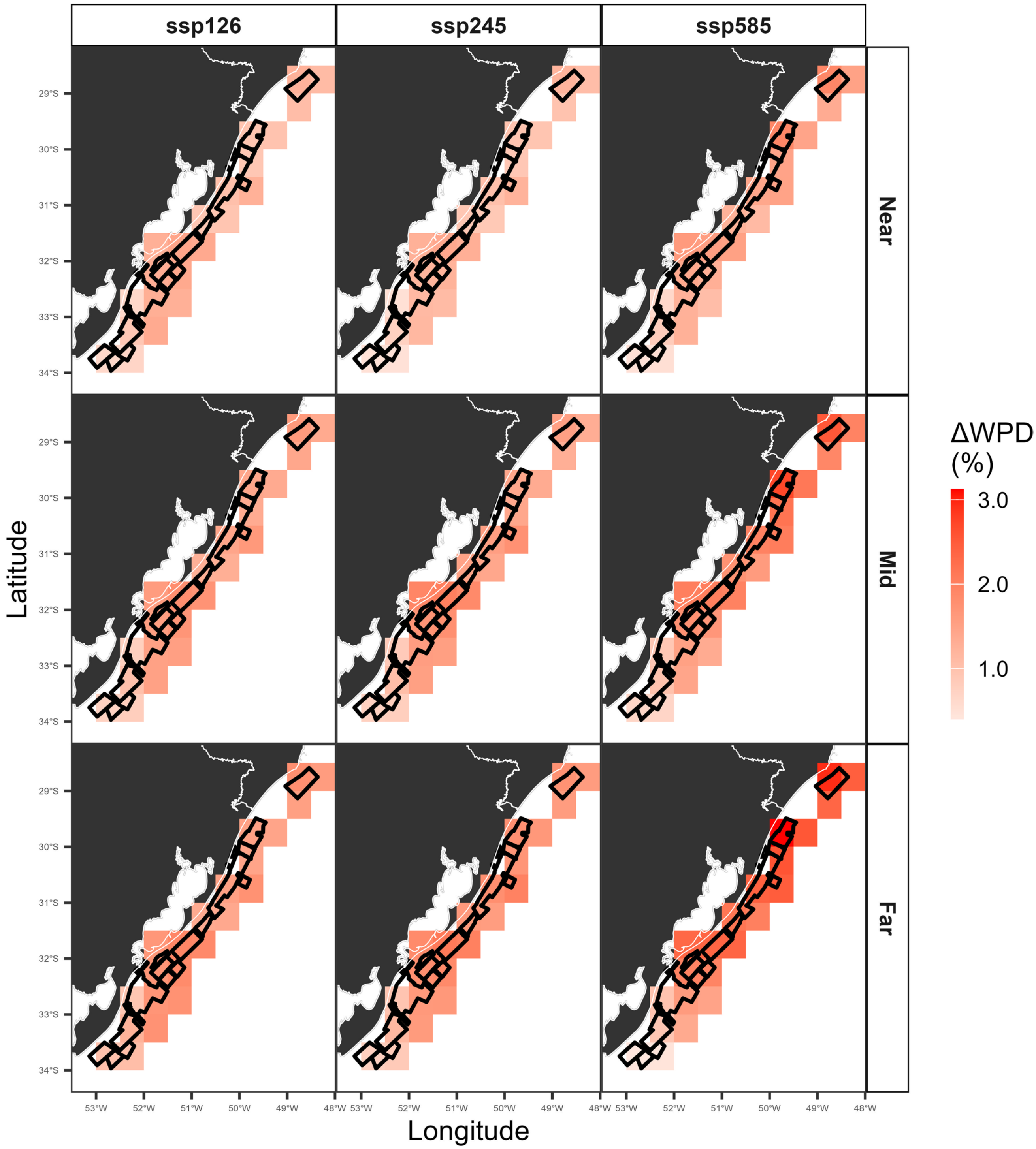

Fig. 9 Same as Fig. 7, but for the offshore region of Southern Brazil

between + 0.5% and + 1.0% in the near future, rising to approximately + 1.0% to + 1.5% in the mid-century period, and stabilizing around + 1.5% in the far future. Under the high-emission scenario SSP5-8.5, a more pronounced upward trend is evident from the outset: increases range between + 1.0% and + 1.5% in the near future, evolving to + 1.5% to + 2.0% in the mid-century period. By the end of the century, projected increases become more substantial, reaching approximately + 2.5% to + 3.0%, with the largest values concentrated in offshore areas south of Rio Grande do Sul and Santa Catarina.

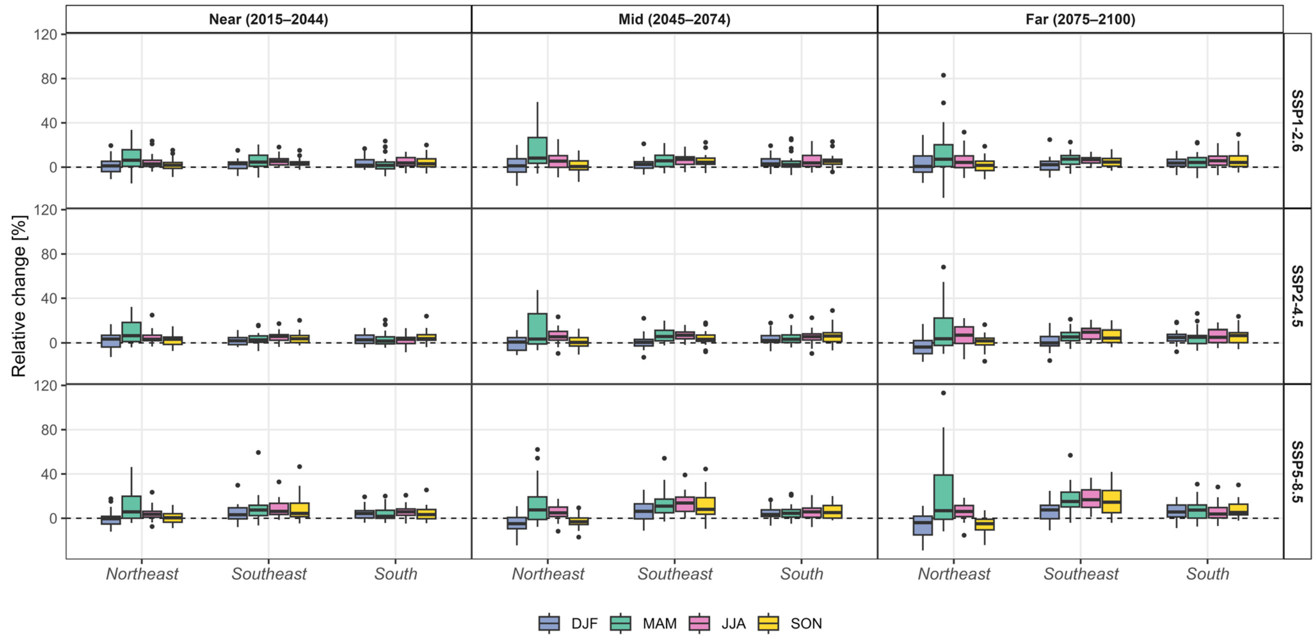

Fig. 10 Seasonal relative change in wind power density (WPD, %) over the Northeast, Southeast, and South regions of Brazil relative to the 1995–2014 reference period. Results are shown for SSP1-2.6, SSP2-4.5, and SSP5-8.5 scenarios (rows) and three future periods: near (2015–2044), mid (2045–2074), and far (2075–2100) (columns). Each boxplot represents the regional seasonal ensemble distribution (DJF, MAM, JJA, SON); the central line indicates the median, boxes the interquartile range, and points the extremes. The dashed line at 0% indicates no change relative to the historical period

This pattern of progressive increase is consistent with regional projections based on dynamical downscaling, which indicate enhanced wind power density in southern Brazil under high-emission scenarios (Reboita et al. 2018), although the magnitudes obtained here are more conservative. Mesoscale modeling studies in the southern Exclusive Economic Zone (Tuchtenhagen et al. 2020) did not identify a robust linear trend during the recent historical period but highlighted strong interannual variability and intensification of extremes. The presence of moderate percentage increases combined with high interannual variability in this study suggests that the projected climate signal remains comparable to the magnitude of natural variability, reinforcing the need for probabilistic approaches in energy applications.

As in the Southeast, SSP5-8.5 yields the largest projected increases, particularly in the mid- and far-future periods. Under this scenario, WPD values become higher and more spatially continuous, indicating greater sensitivity of regional wind resources under stronger radiative forcing. Climate assessments suggest that changes in the Southern Hemisphere westerly wind belt may lead to regional modifications in wind regimes under intensified warming (IPCC 2023a, b). The largest increases are concentrated in offshore areas of southern Santa Catarina and northern Rio Grande do Sul, regions that also exhibit strong seasonal complementarity with Brazil's hydropower system (Silva et al. 2016).

However, the percentage increases projected here are lower than those reported by Reboita et al. (2018), who indicated increases exceeding 100% in wind power density at some locations in southern Brazil under RCP8.5. This difference reinforces that estimates based on high-resolution regional models may amplify the climate signal, whereas the CMIP6 global multi-model ensemble tends to produce more conservative and spatially smoother responses.

Figure 10 presents the relative variation (%) in WPD using boxplots of seasonal ensemble changes for each region × scenario × period combination. Each box summarizes the variability of projected changes within the respective region. The Northeast exhibits extreme variations during the MAM season (March–May), with median increases exceeding + 40% and the presence of outliers ranging from + 80% to + 120% under SSP5-8.5. In contrast, the DJF (December–February) and SON (September–November) seasons show reductions in the far future under the same scenario, with median values between − 10% and − 20%, indicating a seasonal redistribution of the resource rather than a simple shift in annual mean conditions.

For the Southeast, SSP5-8.5 in the far future projects consistent increases across all seasons, with median gains ranging from + 10% to + 25%, particularly pronounced during MAM, JJA (June–August), and SON. In the South, increases are more moderate: under SSP5-8.5 (far future), median changes range between + 5% and + 10%, with stronger signals in JJA and SON. Additionally, boxplots in the South are more compact, indicating lower inter-model spread and greater agreement among projections.

Consistent with the previously discussed spatial patterns, the Northeast exhibits mean changes close to zero or slightly positive under lower forcing scenarios (SSP1-2.6 and SSP2-4.5), particularly in the near future. However, under SSP5-8.5 and toward mid- and far-future periods, a higher frequency of negative values emerges in some seasons, reflecting the previously identified spatial trend of WPD reduction in parts of the northeastern offshore zone. A positive relative change signal is observed during austral autumn and winter, whereas austral spring—the most critical season for wind energy production in the Northeast—shows a systematic reduction over time. The seasonal importance of spring for the northeastern wind regime has been highlighted in hydro-wind complementarity studies (Silva et al. 2016). The projected springtime reduction contrasts with increases reported by Pereira et al. (2013) during autumn and with the spring intensification identified by Reboita et al. (2018) under RCP8.5. This discrepancy highlights the sensitivity of seasonal responses to methodological choices and model configurations, reinforcing the importance of multi-model ensemble approaches to reduce structural uncertainties.

In the Southeast, boxplots indicate a predominance of positive changes across all seasons and scenarios. The increase becomes more pronounced under SSP5-8.5, particularly in the mid- and far-future periods, consistent with spatial patterns showing intensification of wind potential in offshore areas between Rio de Janeiro and Espírito Santo, as well as with multi-model ensemble projections indicating stronger regional contrasts under high-emission scenarios (Ferreira et al. 2024). In the South, a similar pattern to that observed in the Southeast is evident, with predominantly positive values and progressive intensification throughout the century, particularly under SSP5-8.5. This behavior aligns with the previously identified spatial amplification of WPD in offshore areas of southern Santa Catarina and northern Rio Grande do Sul.

4 Conclusions

In summary, offshore wind potential in Brazil does not exhibit a uniform intensification signal under climate change. Instead, the results reveal a spatially heterogeneous and scenario-dependent response. While the Southeast and South show consistent increases in wind power density, particularly under high-emission scenarios, the Northeast, despite maintaining the highest absolute values, may experience localized reductions and significant seasonal redistribution of the resource.

These findings highlight that climate change impacts on wind energy are not limited to changes in mean conditions, but also involve shifts in seasonal dynamics. In the Brazilian context, this is particularly relevant due to hydro-wind complementarity, as reductions during critical seasons, such as austral spring in the Northeast, may affect the balance between wind and hydropower generation.

From a planning perspective, the results suggest that offshore wind expansion strategies in Brazil should account for both current resource availability and projected regional and seasonal changes. The identification of emerging high-potential areas in the Southeast, alongside potential reductions in parts of the Northeast under high-emission scenarios, reinforces the need to integrate climate projections into long-term infrastructure planning, investment decisions, and regulatory frameworks.

More broadly, this study demonstrates that the energy transition must be designed not only as a mitigation pathway but also as a climate-resilient system. The integration of multi-model climate projections, bias correction techniques, and regulatory-relevant spatial domains provides a robust framework for supporting strategic decision-making in offshore wind development.

While wind power density provides a robust first-order estimate of wind energy potential, translating these changes into actual electricity generation requires the integration of turbine-specific power curves and operational constraints. Future work will focus on incorporating representative turbine models to estimate capacity factors and power generation, enabling a more direct assessment of the implications of climate change for offshore wind energy production.

Although the present study focuses on projected changes in mean wind resources and wind power density, climate change may also influence the extreme wind conditions that govern wind turbine design and structural performance. Current wind turbine design standards are largely based on historical wind climate assumptions (IEC 2019), while recent studies have shown that climate change may modify climatic actions and long-term structural reliability, raising important questions regarding the adequacy of existing design criteria under non-stationary climate conditions (Croce et al. 2019). Emerging research further suggests that climate-induced changes in extreme wind hazards may affect design-level wind characteristics, structural safety, and the resilience of wind energy infrastructure (Li 2023; Li and Kopp 2023). In addition, reliability-based approaches have long been recognized as a fundamental framework for evaluating wind turbine performance under ultimate and fatigue loading conditions, providing a rational basis for assessing failure risk and structural safety (Toft and Sørensen 2011). These findings highlight an important research gap, as assessments of future wind energy potential have traditionally emphasized changes in resource availability and power generation, with comparatively less attention given to structural design implications, reliability assessment, and risk evaluation.

Future research efforts will therefore focus on the assessment of extreme wind conditions, particularly in regions identified here as sensitive to climate change signals. Integrating projections of wind resources with analyses of extreme wind hazards, turbine design loads, and structural reliability will provide a more comprehensive framework for evaluating the long-term resilience of offshore wind energy systems under climate change.

Acknowledgements The authors would like to thank the National Council for Scientific and Technological Development (CNPq) and the Coordenação de Aperfeiçoamento de Pessoal de Nível Superior—Brasil (CAPES) for the financial support of this research (Financing Code 001).

Funding The Article Processing Charge (APC) for the publication of this research was funded by the Coordenação de Aperfeiçoamento de Pessoal de Nível Superior - Brasil (CAPES) (ROR identifier: 00x0ma614). The Article Processing Charge (APC) for the publication of this research was funded by the Coordenação de Aperfeiçoamento de Pessoal de Nível Superior—Brasil (CAPES).

Data Availability The data used in this study are publicly available and can be easily accessed on the Copernicus Programme website.

Declarations

Conflict of Interest The authors declare that they have no competing financial interests or personal relationships that could have influenced this article.

Open Access This article is licensed under a Creative Commons Attribution 4.0 International License, which permits use, sharing, adaptation, distribution and reproduction in any medium or format, as long as you give appropriate credit to the original author(s) and the source, provide a link to the Creative Commons licence, and indicate if changes were made. The images or other third party material in this article are included in the article's Creative Commons licence, unless indicated otherwise in a credit line to the material. If material is not included in the article's Creative Commons licence and your intended use is not permitted by statutory regulation or exceeds the permitted use, you will need to obtain permission directly from the copyright holder. To view a copy of this licence, visit http://creativecommons.org/licenses/by/4.0/.

References

Admasu LM, Grant L, Thiery W (2023) Exploring global climate model downscaling based on tile-level output. J Appl Meteorol Climatol 62:171–190. https://doi.org/10.1175/JAMC-D-21-0265.1

International Energy Agency (IEA) (2025) Renewables 2025, IEA, Paris, Licence: CC BY 4.0. Available at: https://www.iea.org/reports/renewables-2025

Archer CL, Jacobson MZ (2005) Evaluation of global wind power. J Geophys Res D Atmos 110:1–20. https://doi.org/10.1029/2004JD005462

Bader DC, Covey C, Gutowski WJ, et al (2008) Climate Models: An Assessment of Strengths and Limitations. Washington, D.C.

Ballarin AS, Sone JS, Gesualdo GC et al (2023) CLIMBra - climate change dataset for Brazil. Sci Data 10:47. https://doi.org/10.1038/s41597-023-01956-z

Bao Y, Song Z, Qiao F (2020) FIO-ESM version 2.0: model description and evaluation. J Geophys Res Oceans. https://doi.org/10.1029/2019JC016036

Bertram C, Brutschin E, Drouet L et al (2024) Feasibility of peak temperature targets in light of institutional constraints. Nat Clim Chang 14:954–960. https://doi.org/10.1038/s41558-024-02073-4

Bi D, Dix M, Marsland S et al (2020) Configuration and spin-up of ACCESS-CM2, the new generation Australian community climate and earth system simulator coupled model. J South Hemisph Earth Syst Sci 70:225–251. https://doi.org/10.1071/ES19040

Boucher O, Servonnat J, Albright AL et al (2020) Presentation and evaluation of the IPSL-CM6A-LR climate model. J Adv Model Earth Syst. https://doi.org/10.1029/2019MS002010

Burton T, Jenkins N, Sharpe D, Bossanyi E (2011) Wind energy handbook. Wiley

Byun Y-H, Lim Y-J, Sung HM et al (2019) NIMS-KMA KACE1.0-G model output prepared for CMIP6 CMIP historical. Earth System Grid Federation. https://doi.org/10.22033/ESGF/CMIP6.8378

Calvin K, Dasgupta D, Krinner G et al (2023) IPCC, 2023: Climate Change 2023: Synthesis Report, Summary for Policymakers. Contribution of Working Groups I, II and III to the Sixth Assessment Report of the Intergovernmental Panel on Climate Change [Core Writing Team, H. Lee and J. Romero (eds.)]. IPCC, Geneva, Switzerland

Cannon AJ, Sobie SR, Murdock TQ (2015) Bias correction of GCM precipitation by quantile mapping: how well do methods preserve changes in quantiles and extremes? J Clim 28:6938–6959. https://doi.org/10.1175/JCLI-D-14-00754.1

Cao J, Wang B, Yang YM et al (2018) The NUIST Earth System Model (NESM) version 3: description and preliminary evaluation. Geosci Model Dev 11:2975–2993. https://doi.org/10.5194/gmd-11-2975-2018

Cherchi A, Fogli PG, Lovato T et al (2019) Global mean climate and main patterns of variability in the CMCC-CM2 coupled model. J Adv Model Earth Syst 11:185–209. https://doi.org/10.1029/2018MS001369

Chipangamate NS, Nwaila GT (2024) Assessment of challenges and strategies for driving energy transitions in emerging markets: a socio-technological systems perspective. Energy Geosci. https://doi.org/10.1016/j.engeos.2023.100257

Croce P, Formichi P, Landi F (2019) Climate change: impacts on climatic actions and structural reliability. Appl Sci (Basel) 9(24):5416. https://doi.org/10.3390/app9245416

Da Silva GK, Dos Santos ACS, Da Silva MVM et al (2017) Estudo dos padrões de ventos offshore no litoral do ceará utilizando dados estimados pelo produto de satélites BSW. Revista Brasileira De Meteorologia 32:579–690. https://doi.org/10.1590/0102-7786324015

Danabasoglu G, Lamarque J-F, Bacmeister J et al (2020) The Community Earth System Model Version 2 (CESM2). J Adv Model Earth Syst. https://doi.org/10.1029/2019MS001916

de Assis Tavares LF, Shadman M, de Freitas Assad LP et al (2020) Assessment of the offshore wind technical potential for the Brazilian Southeast and South regions. Energy (Oxford). https://doi.org/10.1016/j.energy.2020.117097

de Assis Tavares LF, Shadman M, Assad LPdeF, Estefen SF (2022) Influence of the WRF model and atmospheric reanalysis on the offshore wind resource potential and cost estimation: a case study

for Rio de Janeiro State. Energy (Oxford) 240:122767. https://doi.org/10.1016/j.energy.2021.122767
De Castro BM, De Miranda LB (1998) Physical oceanography of the Western Atlantic continental shelf located between 4° N and 34° S (4, W). The sea (ideas and observations on progress in the study of the seas). John Wiley & Sons, New York
de Castro M, Costoya X, Salvador S et al (2019) An overview of offshore wind energy resources in Europe under present and future climate. Ann N Y Acad Sci 1436:70–97
de Freitas IGF, Gomes HB, Peña M et al (2022) Evaluation of wind and wave estimates from CMEMS reanalysis for Brazil's offshore energy resource assessment. Wind Energy 2:586–598. https://doi.org/10.3390/wind2030031
de Lucena AFP, Szklo AS, Schaeffer R, Dutra RM (2010) The vulnerability of wind power to climate change in Brazil. Renew Energy 35:904–912. https://doi.org/10.1016/j.renene.2009.10.022
Dee DP, Uppala SM, Simmons AJ et al (2011) The ERA-Interim reanalysis: configuration and performance of the data assimilation system. Q J R Meteorol Soc 137:553–597. https://doi.org/10.1002/qj.828
dos Reis J, Bose N, Amorim A et al (2023) Wind and solar energy generation potential features in the extreme northern Amazon using reanalysis data. Energies 16:7671. https://doi.org/10.3390/en16227671
DTU Wind (2025) Global Wind Atlas 4.0. Lyngby, Denmark
Dunne JP, Horowitz LW, Adcroft AJ et al (2020) The GFDL Earth System Model Version 4.1 (GFDL-ESM 4.1): overall coupled model description and simulation characteristics. J Adv Model Earth Syst. https://doi.org/10.1029/2019MS002015
Empresa de Pesquisa Energética (EPE) (2024a) Balanço Energético Nacional 2024: Ano base 2023
Empresa de Pesquisa Energética (EPE) (2024b) Plano Decenal de Expansão de Energia 2034
Eyring V, Bony S, Meehl GA et al (2016) Overview of the Coupled Model Intercomparison Project Phase 6 (CMIP6) experimental design and organization. Geosci Model Dev 9:1937–1958. https://doi.org/10.5194/gmd-9-1937-2016
Ferreira GWS, Reboita MS, Ribeiro JGM et al (2024) Assessment of the wind power density over South America simulated by CMIP6 models in the present and future climate. Clim Dyn 62:1729–1763. https://doi.org/10.1007/s00382-023-06993-3
Gan MA, Rao VB (1991) Surface cyclogenesis over South America. Mon Weather Rev 119:1293–1302. https://doi.org/10.1175/1520-0493(1991)119%3c1293:SCOSA%3e2.0.CO;2
Gillett NP, Shiogama H, Funke B et al (2016) The Detection and Attribution Model Intercomparison Project (DAMIP v1.0) contribution to CMIP6. Geosci Model Dev 9:3685–3697. https://doi.org/10.5194/gmd-9-3685-2016
Global Wind Energy Council (2025) Global wind report 2025. Clean
Guimarães RV, Shadman M, Silva SR et al (2025) Cost breakeven point of offshore wind energy in Brazil. Energies (Basel). https://doi.org/10.3390/en18092198
Gurgel AdeRC, Sales DC, Lima KC (2024) Wind power density in areas of Northeastern Brazil from regional climate models for a recent past. PLoS ONE 19:e0307641. https://doi.org/10.1371/journal.pone.0307641
Hajima T, Watanabe M, Yamamoto A et al (2020) Development of the MIROC-ES2L Earth system model and the evaluation of biogeochemical processes and feedbacks. Geosci Model Dev 13:2197–2244. https://doi.org/10.5194/gmd-13-2197-2020
Hersbach H, Bell B, Berrisford P et al (2020) The ERA5 global reanalysis. Q J R Meteorol Soc 146:1999–2049. https://doi.org/10.1002/qj.3803
Hosius E, Seebaß JV, Wacker B, Schlüter JC (2023) The impact of offshore wind energy on Northern European wholesale electricity prices. Appl Energy 341:1120910
IEC (2019) 61400–1: Wind Energy Generation Systems – Part 1: Design Requirements, Pub. L. No. 4th Edition
Intergovernmental Panel on Climate Change (IPCC) (2023b) Climate change 2021 – the physical science basis. Cambridge University Press
Intergovernmental Panel on Climate Change (IPCC) (2023a) Climate change 2022 - mitigation of climate change. Cambridge University Press
International Energy Agency (2024) Renewables 2023. IEA, Paris. Available at: https://www.iea.org/reports/renewables-2023
International Renewable Energy Agency (2024) Renewable Power Generation Costs in 2023. International Renewable Energy Agency, Abu Dhabi. ISBN 978-92-9260-621-3. Available at: https://www.irena.org/Publications/2024/Sep/Renewable-Power-Generation-Costs-in-2023
Kawai H, Yukimoto S, Koshiro T et al (2019) Significant improvement of cloud representation in the global climate model MRI-ESM2. Geosci Model Dev 12:2875–2897. https://doi.org/10.5194/gmd-12-2875-2019
Kelley M, Schmidt GA, Nazarenko LS et al (2020) GISS-E2.1: configurations and climatology. J Adv Model Earth Syst. https://doi.org/10.1029/2019MS002025
Lange S (2019) Trend-preserving bias adjustment and statistical downscaling with ISIMIP3BASD (v1.0). Geosci Model Dev 12:3055–3070. https://doi.org/10.5194/gmd-12-3055-2019
Lee M, Lu M, Im E, Bae D (2019) Added value of dynamical downscaling for hydrological projections in the Chungju Basin, Korea. Int J Climatol 39:516–531. https://doi.org/10.1002/joc.5825
Lee WL, Wang YC, Shiu CJ et al (2020) Taiwan earth system model version 1: description and evaluation of mean state. Geosci Model Dev 13:3887–3904. https://doi.org/10.5194/gmd-13-3887-2020
Li SH (2023) Impact of climate change on wind energy across North America under climate change scenario RCP8.5. Atmos Res 288:106722. https://doi.org/10.1016/j.atmosres.2023.106722
Li SH, Kopp GA (2023) Duration of extreme synoptic wind speeds for North America in a changing climate and its engineering implementation. Struct Saf 104:102349. https://doi.org/10.1016/j.strusafe.2023.102349
Lima DKS, Leão RPS, dos Santos ACS et al (2015) Estimating the offshore wind resources of the State of Ceará in Brazil. Renew Energy 83:203–221. https://doi.org/10.1016/j.renene.2015.04.025
Lin B, Okoye JO (2023) Towards renewable energy generation and low greenhouse gas emission in high-income countries: performance of financial development and governance. Renew Energy 215:118931. https://doi.org/10.1016/j.renene.2023.118931
Linsenmeier M (2023) Temperature variability and long-run economic development. J Environ Econ Manage 121:102840. https://doi.org/10.1016/j.jeem.2023.102840
Mabel MC, Fernandez E (2009) Estimation of energy yield from wind farms using artificial neural networks. IEEE Trans Energy Convers 24:459–464. https://doi.org/10.1109/TEC.2008.2001458
Manwell JF, McGowan JG, Rogers AL (2010) Wind energy explained: theory, design and application
Maraun D (2016) Bias correcting climate change simulations - a critical review. Curr Clim Change Rep 2:211–220
Maraun D, Shepherd TG, Widmann M, et al (2017) Towards process-informed bias correction of climate change simulations. In: Nature Climate Change. Nature Publishing Group, pp 764–773
Martinez A, Iglesias G (2021) Wind resource evolution in Europe under different scenarios of climate change characterised by the novel Shared Socioeconomic Pathways. Energy Convers Manag. https://doi.org/10.1016/j.enconman.2021.113961
Mauritsen T, Bader J, Becker T et al (2019) Developments in the MPI-M Earth System Model version 1.2 (MPI-ESM1.2) and its response to increasing CO2. J Adv Model Earth Syst 11:998–1038. https://doi.org/10.1029/2018MS001400

Meehl GA, Boer GJ, Covey C et al (1997) Intercomparison makes for a better climate model. Eos Trans Am Geophys Union 78:445–451
Miao H, Xu H, Huang G, Yang K (2023) Evaluation and future projections of wind energy resources over the Northern Hemisphere in CMIP5 and CMIP6 models. Renew Energy 211:809–821. https://doi.org/10.1016/j.renene.2023.05.007
Mishra V, Bhatia U, Tiwari AD (2020) Bias-corrected climate projections for South Asia from Coupled Model Intercomparison Project-6. Sci Data 7:338. https://doi.org/10.1038/s41597-020-00681-1
Moradian S, Akbari M, Iglesias G (2022) Optimized hybrid ensemble technique for CMIP6 wind data projections under different climate-change scenarios. Case study: United Kingdom. Sci Total Environ. https://doi.org/10.1016/j.scitotenv.2022.154124
Mukherjee S, Aadhar S, Stone D, Mishra V (2018) Increase in extreme precipitation events under anthropogenic warming in India. Weather Clim Extrem 20:45–53. https://doi.org/10.1016/j.wace.2018.03.005
Nizamani Z et al (2024) Renewable wind energy resources in offshore low wind speeds regions near the equator: a review. Ocean Eng 311:118834. https://doi.org/10.1016/j.oceaneng.2024.118834
Nóbrega ADS (2025) Estudo sobre a construção econômico-política da rede de produção de energia eólica no Brasil. Revista Brasileira De Planejamento e Desenvolvimento 14(1):66–96. https://doi.org/10.3895/rbpd.v14n1.17262
Nogueira EC, Morais RC, Pereira AO (2023) Offshore Wind Power Potential in Brazil: Complementarity and Synergies. Energies (Basel). https://doi.org/10.3390/en16165912
ONS – Operador Nacional do Sistema Elétrico (2025) Dados de capacidade instalada de geração eólica. https://www.ons.org.br/paginas/resultados-da-operacao/boletim-geracao-eolica.aspx. Accessed 29 Aug 2025
International Renewable Energy Agency and International Labour Organization (IRENA and ILO) (2026) Renewable energy and jobs: Annual review 2025, International Renewable Energy Agency, Abu Dhabi; and International Labour Organization, Geneva. Available at: https://www.irena.org/-/media/Files/IRENA/Agency/Publication/2026/Jan/IRENA_SOC_RE_and_jobs_2026.pdf
Pak G, Noh Y, Lee M-I et al (2021) Korea Institute of Ocean Science and Technology Earth System Model and its simulation characteristics. Ocean Sci J 56:18–45. https://doi.org/10.1007/s12601-021-00001-7
Pallabazzer R (1995) Evaluation of wind-generator potentiality. Sol Energy 55:49–59. https://doi.org/10.1016/0038-092X(95)00040-X
Pallabazzer R (2004) Previsional estimation of the energy output of windgenerators. Renew Energy 29:413–420. https://doi.org/10.1016/S0960-1481(03)00197-6
Pereira EB, Martins FR, Pes MP et al (2013) The impacts of global climate changes on the wind power density in Brazil. Renew Energy 49:107–110. https://doi.org/10.1016/j.renene.2012.01.053
Peterson EW, Hennessey JP (1978) On the Use of Power Laws for Estimates of Wind Power Potential. J Appl Meteorol Climatol 17:390–394. https://doi.org/10.1175/1520-0450(1978)017%3C0390:OTUOPL%3E2.0.CO;2
Pimenta F, Kempton W, Garvine R (2008) Combining meteorological stations and satellite data to evaluate the offshore wind power resource of Southeastern Brazil. Renew Energy 33:2375–2387. https://doi.org/10.1016/j.renene.2008.01.012
Pryor SC, Barthelmie RJ (2010) Climate change impacts on wind energy: a review. Renew Sustain Energy Rev 14:430–437
Pryor SC, Barthelmie RJ (2013) Assessing the vulnerability of wind energy to climate change and extreme events. Clim Change 121:79–91. https://doi.org/10.1007/s10584-013-0889-y
Pryor SC, Coburn JJ, Barthelmie RJ, Shepherd TJ (2023) Projecting future energy production from operating wind farms in North America. Part I: dynamical downscaling. J Appl Meteorol Climatol 62:63–80. https://doi.org/10.1175/JAMC-D-22-0044.1
Reboita MS, Amaro TR, de Souza MR (2018) Winds: intensity and power density simulated by RegCM4 over South America in present and future climate. Clim Dyn 51:187–205. https://doi.org/10.1007/s00382-017-3913-5
Reboita M, Kiani R, Ali S, Khan T (2021) Projections of wind power density in Pakistan and adjacent regions. Clim Res 85:177–192. https://doi.org/10.3354/cr01679
Instituto Brasileiro do Meio Ambiente e dos Recursos Naturais Renováveis (IBAMA) (2020) Termo de Referência - Estudo de Impacto Ambiental e Relatório de Impacto Ambiental EIA/Rima
Instituto Brasileiro do Meio Ambiente e dos Recursos Naturais Renováveis (IBAMA) (2022) Mapas de projetos em licenciamento - Complexos Eólicos Offshore
Instituto Brasileiro do Meio Ambiente e dos Recursos Naturais Renováveis (IBAMA) (2025) Ibama emite 1ª licença prévia para projeto eólico offshore no Brasil. Instituto Brasileiro do Meio Ambiente e dos Recursos Naturais Renováveis. https://www.gov.br/ibama/pt-br/assuntos/noticias/2025/ibama-emite-1a-licenca-previa-para-projeto-eolico-offshore-no-brasil
Instituto Brasileiro do Meio Ambiente e dos Recursos Naturais Renováveis (IBAMA) (2026) Offshore wind projects in licensing – spatial dataset (February 2026). Available at: https://www.gov.br/ibama/pt-br/assuntos/laf/consultas/arquivos/20260303_Eolicas_Offshore_Ibama_fevereiro_26.pdf. Accessed May 2026
Instituto Brasileiro do Meio Ambiente e dos Recursos Naturais Renováveis (IBAMA) (2026) Offshore wind projects under environmental licensing. Available at: https://www.gov.br/ibama/pt-br/assuntos/laf/consultas/mapas-de-projetos-em-licenciamento-complexos-eolicos-offshore. Accessed May 2026
Riahi K, van Vuuren DP, Kriegler E et al (2017) The Shared Socioeconomic Pathways and their energy, land use, and greenhouse gas emissions implications: an overview. Glob Environ Change 42:153–168. https://doi.org/10.1016/j.gloenvcha.2016.05.009
Rong X, Li J, Chen H et al (2018) The CAMS climate system model and a basic evaluation of its climatology and climate variability simulation. J Meteorol Res 32:839–861. https://doi.org/10.1007/s13351-018-8058-x
Séférian R, Nabat P, Michou M et al (2019) Evaluation of CNRM Earth System Model, CNRM-ESM2-1: role of Earth System Processes in present-day and future climate. J Adv Model Earth Syst 11:4182–4227. https://doi.org/10.1029/2019MS001791
Seland Ø, Bentsen M, Olivié D et al (2020) Overview of the Norwegian Earth System Model (NorESM2) and key climate response of CMIP6 DECK, historical, and scenario simulations. Geosci Model Dev 13:6165–6200. https://doi.org/10.5194/gmd-13-6165-2020
Sellar AA, Jones CG, Mulcahy JP et al (2019) UKESM1: description and evaluation of the U.K. Earth system model. J Adv Model Earth Syst 11:4513–4558. https://doi.org/10.1029/2019MS001739
Silva JA (2023) Energia eólica no Brasil: avanços e desafios. Princípios 42(167):179–202. https://doi.org/10.4322/principios.2675-6609.2023.167.010
Silva AR, Pimenta FM, Assireu AT, Spyrides MHC (2016) Complementarity of Brazil's hydro and offshore wind power. Renew Sustain Energy Rev 56:413–427
Lee Taesam, Singh VP (2019) Statistical downscaling for hydrological and environmental applications. CRC Press, Taylor & Francis Group
Swart NC, Cole JNS, Kharin VV et al (2019) The Canadian Earth system model version 5 (CanESM5.0.3). Geosci Model Dev 12:4823–4873. https://doi.org/10.5194/gmd-12-4823-2019

Tang G, Clark MP, Papalexiou SM (2022) EM-Earth: the ensemble meteorological dataset for planet Earth. Bull Am Meteorol Soc 103:E996–E1018. https://doi.org/10.1175/BAMS-D-21-0106.1

Tatebe H, Ogura T, Nitta T et al (2019) Description and basic evaluation of simulated mean state, internal variability, and climate sensitivity in MIROC6. Geosci Model Dev 12:2727–2765. https://doi.org/10.5194/gmd-12-2727-2019

Tebaldi C, Knutti R (2007) The use of the multi-model ensemble in probabilistic climate projections. Philos Trans R Soc A Math Phys Eng Sci 365:2053–2075

Toft HS, Sørensen JD (2011) Reliability-based design of wind turbine blades. Struct Saf 33(6):333–342. https://doi.org/10.1016/j.strusafe.2011.05.003

Tran-Anh Q, Ngo-Duc T, Espagne E, Trinh-Tuan L (2023) A 10-km CMIP6 downscaled dataset of temperature and precipitation for historical and future Vietnam climate. Sci Data 10:257. https://doi.org/10.1038/s41597-023-02159-2

Troen LB, Petersen EL (1989) European wind atlas. Risø National Laboratory

Tuchtenhagen P, de Carvalho GG, Martins G et al (2020) WRF model assessment for wind intensity and power density simulation in the southern coast of Brazil. Energy. https://doi.org/10.1016/j.energy.2019.116341

van Bommel N, Höffken JI (2023) The urgency of climate action and the aim for justice in energy transitions – dynamics and complexity. Environ. Innov. Soc. Transit. 48:100763

Villanueva D, Feijóo A (2010) Wind power distributions: a review of their applications. Renew Sustain Energy Rev 14:1490–1495. https://doi.org/10.1016/j.rser.2010.01.005

Voldoire A, Saint-Martin D, Sénési S et al (2019) Evaluation of CMIP6 DECK experiments with CNRM-CM6-1. J Adv Model Earth Syst 11:2177–2213. https://doi.org/10.1029/2019MS001683

Volodin E, Gritsun A (2018) Simulation of observed climate changes in 1850–2014 with climate model INM-CM5. Earth Syst Dyn 9:1235–1242. https://doi.org/10.5194/esd-9-1235-2018

Wieringa J (1992) Updating the Davenport roughness classification. J Wind Eng Ind Aerodyn 41:357–368. https://doi.org/10.1016/0167-6105(92)90434-C

Wilks DS (2020) Statistical methods in the atmospheric sciences, Fourth. Elsevier

Williams KD, Copsey D, Blockley EW et al (2018) The Met Office global coupled model 3.0 and 3.1 (GC3.0 and GC3.1) configurations. J Adv Model Earth Syst 10:357–380. https://doi.org/10.1002/2017MS001115

Wu H, Lei H, Lu W, Liu Z (2022) Future changes in precipitation over the upper Yangtze River basin based on bias correction spatial downscaling of models from CMIP6. Environ Res Commun 4:045002. https://doi.org/10.1088/2515-7620/ac620e

Xiao-Ge XIN, Tong-Wen WU, Jie ZHANG et al (2019) Introduction of BCC models and its participation in CMIP6. Climate Change Research 15:533–539

Xu Z, Han Y, Tam C-Y et al (2021) Bias-corrected CMIP6 global dataset for dynamical downscaling of the historical and future climate (1979–2100). Sci Data 8:293. https://doi.org/10.1038/s41597-021-01079-3

Zakari Y, Michel A, Lehning M (2022) Future trends in wind resources and their consistency in the Indian sub-continent. Sustain Energy Technol Assess 53:102460. https://doi.org/10.1016/j.seta.2022.102460

Zhang S, Li X (2021) Future projections of offshore wind energy resources in China using CMIP6 simulations and a deep learning-based downscaling method. Energy 217:119321. https://doi.org/10.1016/j.energy.2020.119321

Zhang Z, Zhang G, Li L (2023) The spatial impact of atmospheric environmental policy on public health based on the mediation effect of air pollution in China. Environ Sci Pollut Res 30:116584–116600. https://doi.org/10.1007/s11356-022-21501-6

Zhou TJ, Wang B, Yu YQ et al (2018) The FGOALS climate system model as a modeling tool for supporting climate sciences: an overview. Earth Planet Phys 2:276–291

Ziehn T, Chamberlain MA, Law RM et al (2020) The Australian earth system model: ACCESS-ESM1.5. J South Hemisph Earth Syst Sci 70:193–214. https://doi.org/10.1071/ES19035

Publisher's Note Springer Nature remains neutral with regard to jurisdictional claims in published maps and institutional affiliations.